

1N-44-69358

DOE/JPL-956289-86/1
9950-1234

P 87

HIGH EFFICIENCY CRYSTALLINE SILICON SOLAR CELLS

(NASA-CR-180530) HIGH EFFICIENCY
CRYSTALLINE SILICCN SOLAR CELLS Final
Technical Report (Jet Propulsion Lab.) 87 p
CSSL 10A

N87-21411

Unclas
G3/44 43555

THIRD TECHNICAL REPORT
FINAL TECHNICAL REPORT

June 15, 1986

By

C. Tang Sah

Contract No. 956289

The JPL Flat-Plate Solar Array (FSA) Project is sponsored by the U. S. Department of Energy (DOE) and forms part of the Photovoltaic Energy Systems Program to initiate a major effort toward the development of cost-competitive solar arrays. This work was performed for the Jet Propulsion Laboratory, California Institute of Technology, and the U.S. Department of Energy, through an agreement between the National Aeronautics and Space Administration and the Department of Energy.

DOE/JPL-956289-86/1
Dist.Category UC-63

HIGH EFFICIENCY CRYSTALLINE SILICON SOLAR CELLS

THIRD TECHNICAL REPORT
FINAL TECHNICAL REPORT

June 15, 1986

By

C. Tang Sah

Contract No. 956289

The JPL Flat-Plate Solar Array (FSA) Project is sponsored by the U. S. Department of Energy (DOE) and forms part of the Photovoltaic Energy Systems Program to initiate a major effort toward the development of cost-competitive solar arrays. This work was performed for the Jet Propulsion Laboratory, California Institute of Technology, and the U.S. Department of Energy, through an agreement between the National Aeronautics and Space Administration and the Department of Energy.

ABSTRACT

A review of the entire research program since its inception ten years ago is given in this final report. The initial effort focused on the effects of impurities on the efficiency of silicon solar cells to provide figures of maximum allowable impurity density for efficiencies up to about 16 to 17% (AM1). Highly accurate experimental techniques (Capacitance Transient Spectroscopy) were extended to characterize the recombination properties of the residual impurities in silicon solar cell. A novel numerical simulator of solar cell was also developed, using the Circuit Technique for Semiconductor Analysis, which has provided exact theoretical design criteria on the maximum allowable impurity density. Recent effort until the end of this program has focused on the delineation of the material and device parameters which limited the silicon AM1 efficiency to below 20% and on an investigation of cell designs to break the 20% barrier. It is shown that the known and newly proposed high efficiency design criteria, if all implemented successful in one cell, could give AM1 efficiencies of 20% or higher. These include implementing a thin graded-base back-surface-field by epitaxy, minimizing emitter contact and surface or interface recombination losses using high/low emitter junctions, removing junction perimeter recombination losses, and maintaining a high base lifetime. Fabrication of such a cell has not been reported although an earlier cell design of Green came closest without using a graded base nor special perimeter loss reduction. Novel designs of the cell device structure and geometry can further reduce recombination losses as well as the sensitivity and criticalness of the fabrication technology required to exceed 20%. These include texturized-grooved emitter and reflecting back surface for higher absorption, floating emitter transistor cell to eliminate emitter bulk and surface recombination, and polysilicon emitter and base contact barriers to further reduce emitter contact recombination. These innovative cell designs are essential to reach the fundamental or intrinsic limit of 25% efficiency. It is concluded that the practical limitation in silicon cells with efficiency substantially higher than 20% comes from recombination of the photogenerated carriers at the residual impurity and defect recombination centers in the base. This calls for further research on the fundamental characterization of the carrier recombination properties at the chemical impurity and physical defect centers. It is further shown that only single crystalline silicon cell technology can be successful in attaining efficiencies greater than 20%. Other forms, such as polycrystalline silicon and amorphous silicon, are unlikely to exceed 20% efficiency due to the physical defects in these materials, grain boundaries in the former and dangling bonds in the latter, which are efficient recombination sites and which cannot be completely passivated, such as by hydrogen or other neutralizing impurities, in order to reduce the residual active recombination center densities is less than 10^{10} cm^{-3} .

TECHNICAL CONTENT STATEMENT

This report was prepared as an account of work sponsored by the United States Government. Neither the United States nor the United States Department of Energy, nor any of their employees, nor any of their contractors, subcontractors or their employees, makes any warranty, express or implied, or assumes any legal liability or responsibility for the accuracy, completeness or usefulness of any information, apparatus, product or process disclosed, or represents that its use would not infringe privately owned rights.

Reference herein to any specific commercial product, process, or service by trade name, trademark, manufacturer, or otherwise, does not necessarily constitute or imply its endorsement, recommendations, or favoring by the United States Government or any agency thereof. The views and opinions of authors expressed herein do not necessarily state or reflect those of the United States Government or any agency thereof.

NEW TECHNOLOGY

New high efficiency silicon solar cell structures have been reported and disclosed to the office of Patents and Technology Utilizations of the Jet Propulsion Laboratory of California Institute of Technology.

TABLE OF CONTENT

Section	Page
COVER PAGE	-
ABSTRACT	-
TECHNICAL CONTENT STATEMENT	i
NEW TECHNOLOGY STATEMENT	ii
TABLE OF CONTENT	iii
LIST OF ILLUSTRATION	iv
LIST OF TABLE	v
I. INTRODUCTION	1
II. PROGRESSES	3
2.1 THEORETICAL AND EXPERIMENTAL STUDIES OF IMPURITY RECOMBINATION CENTERS (Task 1)	3
2.2 GENERATION OF MATHEMATICAL MODELS (Task 2)	10
2.3 IDENTIFICATION OF EFFICIENCY LIMITING FACTORS AND RECOMMENDATION OF PRACTICAL SOLUTIONS (Task 3) ...	20
2.4 EXPERIMENTAL DEMONSTRATION AND IMPLEMENTATION	27
III. CONCLUSION	28
IV. REFERENCES	32
V. APPENDIX	36
HIGH EFFICIENCY CRYSTALLINE SILICON SOLAR CELLS (Preprint of article to appear in the special issue of Solar Cell, February, 1986. 44 pages.)	

LIST OF ILLUSTRATIONS

There are no illustrations in the main text.
There are several figures in the appendix.

LIST OF TABLES

	page
TABLE I. PERFORMANCE PARAMETERS OF THE IDEAL DIODE SILICON SOLAR CELL (AM1 or AM1.5, 24.0C).	23
TABLE II. PERFORMANCE OF SEVERAL HIGH EFFICIENCY LABORATORY SILICON SOLAR CELLS.	24

I. INTRODUCTION

This program began on July 1, 1982. The first technical manager of the contractor was Dr. Ralph Lutwack of the Jet Propulsion Laboratory. The initial emphasis was on a study of the relations of the material properties and high efficiency solar cell performance on material composition, which was also the contract title. The objectives were covered by two interrelated tasks: (1) theoretical and experimental studies of impurity related energy levels, densities of these levels and electron-hole thermal capture and emission rates at these levels; and (2) generation of mathematical models to describe the experimental results in order to aid in the specification of the material properties and device structures required for very high-efficiency solar cells. Dr. Li-Jen Cheng of the Jet Propulsion Laboratory has served as the second technical manager until the end of the contract, June 15, 1986.

The planning to expand and focus more sharply on the last aspect of task (2) began in August 1983 resulting in the addition of tasks 3 and 4. Task 3 calls for the identification of the factors which limit the AM1 efficiency of silicon solar cells with efficiencies below and above 20% and recommendation of practical solutions to achieve efficiencies greater than 20%. Task 4 concerns experimental demonstration and the practical implementation of the recommended practical solutions.

This is the third and final technical report of this program. In addition to the previous technical reports [1,2] and resulting publications in the open literature [3,4], findings from this program have also been reported at

the High-Efficiency Modeling Workshop on March 13, 1984 [5], the High-Efficiency Crystalline Silicon Solar Cell Research Forum from July 9 to 11, 1984 [6], the 24th, 25th and 26th Project Integration Meetings on October 2, 1984 [7], June 19, 1985 [8] and April 29, 1986 [9] respectively, and the Workshop on Low-Cost Polysilicon for Terrestrial Photovoltaic Solar Cell Applications on October 28, 1985 [10]. New cell structures were proposed in a patent application which was jointly submitted by Chih-Tang Sah and Li-Jen Cheng and filed by the Jet Propulsion Laboratory and NASA with the United States Patent Office in February, 1986 [11].

This final report will present summaries of the results of this program. Progresses are described in the next section, section II. A concluding summary is given in section III. References cited in the text are enclosed by the square bracket [] and a list of references is given in section IV.

II. PROGRESSES

Objectives of the tasks are first given. They are then followed by a description of the progresses made.

2.1 THEORETICAL AND EXPERIMENTAL STUDIES OF IMPURITY RELATED ENERGY LEVELS, LEVEL DENSITIES AND CARRIER CAPTURE RATES. (Task 1)

This task was a continuation of a previous JPL contract whose main objective was to provide accurate and detailed characterization of the recombination properties of residual impurity recombination centers in solar cell grade silicon. That effort was summarized by its program manager, Dr. Ralph Lutwack [12]. The residual impurities are present in the original silicon stock which are not completely removed during the single crystal growth processes, such as the Czochralski and the float-zone techniques and other techniques developed specially for low cost solar cells such as the cast technique. Some of the principal residual impurities which can significantly increase the recombination rates of the photo-generated electrons and holes are the transition metals commonly found in the silicon feed stock, such as Ti, Mo, W and others [13,14]. In addition, recombination impurities can be introduced during refining of silicon feed stock, such as in the zinc reduction process [15]. Impurities such as gold are also introduced, unavoidably, during fabrication even in the most advanced state-of-the-art silicon VLSI production lines.

2.1.1 HISTORICAL SUMMARY

In the early phase of the solar photovoltaic programs which began around 1975, efforts were directed to an investigation of inexpensive solar grade starting silicon material [12] which contains high densities of these residual impurities [13,14]. Silicon purification methods to achieve low cost cells and panels would not allow the complete removal of these residual impurities from the silicon crystals grown from silicon stocks having a high concentration of these impurities. Efficiency were limited to about 15%. In order to assess the importance and the maximum allowable density of these residual impurities for a given cell efficiency in the 15% range, accurate recombination rates of electrons and holes at these residual impurity recombination centers must be known. A focused effort was directed by Jet Propulsion Laboratory [12] to determine the effects of these impurities on the silicon solar cell performance and to provide detailed characterization so that accurate electron-hole recombination parameters at these impurity sites can be obtained. The values of these recombination rates are needed in order to optimize the design of silicon solar cells to reach the lowest manufacturing cost.

The most accurate and sensitive method for the determination of the recombination parameters has been the capacitance and current transient technique pioneered by Sah and his graduate students during 1964 to 1972 [16] which was further refined and improved by his recent graduate students [17-23]. The technique is so sensitive that it can detect the trapping of 2000 electrons or holes trapped at a recombination level in a p/n junction.

During the previous contract, a detailed characterization of the carrier

recombination properties at the zinc center was completed and the maximum allowable zinc concentration at a given cell efficiency was computed [18]. Efforts were also made on the characterization of other impurities which may be present in solar grade silicon, such as Ti and V.

The support of this project was shifted to other sources during the current JPL contract due to redirecting the current efforts to the designs and limiting factor delineation of very high efficiency cells. The decision was based on the incorrect assumptions that in order to reach very high efficiencies, above 20%, these impurities cannot be present even at the part per billion level in the silicon single crystal prior to cell fabrication and that the residual recombination could be from process induced centers introduced during cell fabrication rather than impurities originally present in the starting crystal. Other uncertainties were a concern of the identity of the remaining impurities and on whether it is a chemical impurity or a physical defect (vacancy) or their complexes; but regardless, their presence prevents the efficiency to reach its intrinsic value. The intrinsic value, estimated at 25%-AM1 [2,4,6,10], is limited by non-impurity and non-defect recombinations such as the band-to-band thermal and Auger recombination losses. The concern on uncontrollable random introduction of the impurity recombination center during cell fabrication is quite serious. Even for the cleanest silicon VLSI fabrication facility and production line to date, there is no assurance that the residual recombination impurity level in the final silicon device chip can be kept below a density of 1.0×10^{14} atom/cm³. We have demonstrated [18] that the cell efficiency is limited by electron-hole recombination at the impurity centers even at this low impurity density level. Thus, the question on which recombination impurity or defect that limits a current production silicon cell

to less than 20%, is still an open one. And, to reach efficiencies above 20%, all residual recombination impurity densities must be controlled to a level significantly (one or two orders of magnitudes) below 10^{11} atom/cm³ which is yet to be attainable by the current state-of-the-art silicon VLSI technology.

Thus, the question of residual recombination impurity and defect centers that will limit the efficiency in cells above 20% remains a very important one which must be resolved. Without the detailed recombination parameters, only a blind brute-force and expensive purification and fabrication procedure can be used to reduce recombination losses and there is no assurance that reproducible efficiency greater than 20% can be attained consistently. The importance of continuing the fundamental characterization work, which was the principal objective of the previous contract for cell efficiencies from 10 to 16% or 18% range, should be emphasized again for very high efficiency cell research in order to reach efficiencies above 20%. To date, low cost is yet to be a viable question on cells above 20% since there is no existence proof in one fabricated cell which has been designed and built to take into account of all the currently known high efficiency design considerations. These considerations have already predicted an efficiency greater than 20% in a planar cell structure without the new high-efficiency device innovations.

Due to the redirection and new focus of the current contract, the support of the characterization effort on impurity recombination centers was shifted to other sources in order to continue this valuable research effort. It is continued not only for its anticipated practical importance just stated, but also the fundamental understanding of the recombination mechanisms and rates that can be derived from the careful and detailed measurements. Through the

advance in the fundamental understanding, further design guides can be expected to help attaining very high efficiencies at lower costs. Furthermore, this basic research is continued in order to take advantage of the large number of impurity-doped silicon single crystals carefully grown under controlled conditions by the Westinghouse Research Laboratory under a previous Jet Propulsion Laboratory contract. Our efforts, not supported by the current JPL contract, nevertheless, produced several major breakthroughs on the use of the transient capacitance method to determine the recombination properties of deep-level electron and hole traps. These new methods have made it possible to completely characterize the recombination properties of the zinc and titanium centers which could be important residual impurities in silicon solar cells. These have been reported in journal articles and summarized as follows.

2.1.2 SUMMARY OF BREAKTHROUGHS ON CHARACTERIZATION OF RECOMBINATION CENTERS

The major breakthroughs are summarized in this section. The details are documented in the cited journal articles from which the new measurement procedures can be repeated and the recombination parameters obtained. These are:

- (1) the identification of additional sources of nonexponential transients in the capacitance-versus-time decay curves [19] which showed that an abrupt or sharp change in the density of the recombination centers with position or depth in the p/n junction can give rise to a non-exponential transient even when the recombination density is very low,
- (2) the development and in-depth demonstration of a new variation of the

capacitance transient method which allows the determination of both the majority and minority carrier recombination and capture rates at equilibrium or zero electric field, at a one-level or even two-level recombination center, using only ONE p/n junction diode [17],

(3) the identification of the quantum mechanisms which control the magnitude of the capture and recombination rates of electrons and holes at the two zinc acceptor centers in silicon [20] and the two titanium donor centers in silicon [21], and

(4) the demonstration of the importance of impurity-related recombination at the surface and the interfaces on the accuracy of the measured electron and hole capture and recombination rate coefficients [22].

The new method has also been applied recently to resolve the controversy on the nature and inter-relationship of the two gold levels in silicon showing that the gold acceptor level at the silicon midgap is not related to the phosphorus donor dopant density as suggested by D. Lang but is most likely the isolated substitutional gold center with the neutral binding potential for a hole or an electron [23]. This midgap gold level could be one of the most important residual recombination site in very-high-efficiency (>20%) silicon solar cells since it is well known that a residual amount of gold is still present in the highest purity chemicals used in silicon integrated circuit fabrication.

2.1.3 FUTURE PROSPECTS

To attain very high efficiency, efficiencies greater than 20%, the importance to have detailed complete characterization of the electron and hole recombination properties at traps from both chemical impurities and physical defects cannot be emphasized enough. The previous subsections have given much of the technical bases on the needs for such a complete and in-depth characterization research effort. The current state of the knowledge shows definitely that characterization of recombination centers is at its infancy, but a very promising beginning in view of the powerful new measurement techniques described in the previous subsection. At present, only two impurity centers (zinc and titanium) and no physical defects have been characterized to the level of detail and accuracy required to do first-principle (in contrast to empirical) design optimizations using the exact solar cell computer simulator to be described in the next subsection. Considerable further efforts and careful measurements are necessary for the many chemical-impurity and physical-defect centers which are likely to be responsible for the residual base recombination losses that limit the silicon solar cell efficiency to 20%.

A strong need for compound semiconductor material research, similar to the silicon impurity studies described here, was recognized and emphasized by Dr. Henry Brandhorst of NASA Lewis Research Center in a recent report titled, Issue Study on Multijunction Compound Semiconductor Solar Cells for Concentrators, in space applications [24]. All of the novel and new extensions of the capacitance transient spectroscopy techniques, developed for silicon just described, are directly applicable to the characterization of electron and hole traps in GaAs and related compound semiconductor solar cells.

2.2 GENERATION OF MATHEMATICAL MODELS TO DESCRIBE THE EXPERIMENTAL RESULTS AND TO SPECIFY THE MATERIAL PROPERTY REQUIREMENTS FOR HIGH EFFICIENCY SOLAR CELLS. (Task 2)

There are two parts to this task: (i) formulation of a mathematical model for solar cells and (ii) the application of the model for numerical analysis and simulation of solar cell performance.

2.2.1 MATHEMATICAL MODEL AND COMPUTER SIMULATOR OF SOLAR CELLS

Formulation of the mathematical model and a computer simulator of solar cells were accomplished during the previous contract based on a new numerical technique to be described below. A most versatile solar cell simulator, written in FORTRAN, was developed from existing codes written by us prior to the beginning of the previous contract. This simulator can accurately compute the performances of solar cells of any dopant and recombination impurity profiles using the experimentally measured electron capture and emission rates at the recombination centers in the cell.

The method involves the numerical solution of the six semiconductor or Shockley equations by a new technique, known as the Circuit Technique for Semiconductor Analysis (CTSA, which is also synonymous with C.T. Sah Associates in recognizing the efforts of a group of his former associates and graduate students who had contributed to coding the program based on the circuit model developed by him in a series of about ten articles during 1962 to 1972). For a reference of the details of the development, see the zinc paper [18], the first annual report of the previous contract [25] and a summary given in the invited

high-efficiency paper [4] which is also attached as appendix A. In this technique, the six (or seven if there are two recombination levels in the cell) semiconductor equations are first employed to synthesize two equivalent circuit models, one for the d.c. currents and voltages and one for the small-signal currents and voltages. The latter was originally developed to compute the small-signal impedance or admittance of the device after d.c. convergence is achieved. The small-signal circuit model is also used as the error circuit model to compute the errors in the d.c. voltages or potentials of each node after every iteration cycle. These voltage errors are then used as the corrections to the previous d.c. voltages at each node to give a set of new d.c. voltages which is then used to compute the values of the resistors and capacitors of the circuit elements of the error circuit model. Using these equivalent circuit models, the numerical solution procedure becomes very straight forward - involving the solution of the matrix equations of the error circuit model for each iteration.

There are many obvious advantages of this method compared with the conventional finite difference and finite element methods. (1) All the circuit elements in the small-signal or error circuit model are related to physical processes of diffusion, drift, carrier capture and emission at deep traps or deep levels, and carrier interband generation and recombination. (2) Boundary conditions can be set very easily by shorting, opening or connecting resistors and capacitors to the appropriate nodes, even for highly nonlinear boundary effects, without the need of making any approximations such as that employed in the analytical approaches used in the finite difference and finite element methods. (3) Any geometry can be easily dealt with, either using a rectangular grid or non-rectangular grid with visual pictures of the fundamental transport

processes occurring at each node or grid point. (4) The numerical solution method follows the conventional ones used in finding the roots of a sparse matrix without having to develop any new techniques. (5) Convergence has been very rapid and seldom fails even with poor initial guesses. (6) Small-signal admittances are automatically computed without further efforts after a convergent d.c. solution is obtained. (7) The electrical circuit concepts and the properties of the circuit elements, capacitor, resistor, independent and dependent current and voltage sources, are familiar to engineers and physicists.

As an example, a complete set of current-voltage characteristics of a solar cell at AM1 or another illumination level and the four principal cell performance parameters, VOC, JSC, FF and EFF, can all be obtained in about 60 CPU seconds on a CDC Cyber-175 computer with single (60-bit) precision and at an accuracy of 0.01 mV. This benchmark is obtained for an arbitrary doping impurity profile and another arbitrary recombination center density profile, even if the initial guess is not a highly accurate equilibrium solution of the electric potential distribution. The CPU time could be reduced to 15 seconds or less if the initial guess comes from the illuminated solution of a previously converged solution. The computed results include also the depth variations of all the internal device parameters, such as the recombination rates, the charge states, the density of recombination centers in each charge state, the densities of the trapped electrons or holes at the recombination centers, the band electron and hole densities, the electric field, the electrostatic potential, the quasi-Fermi potentials of electrons and holes, and the net space-charge density.

2.2.2 APPLICATIONS OF THE CTSA SOLAR CELL SIMULATOR

The second objective involved the application of this solar cell simulator to exploit the various material and device geometry combinations that may improve or limit the efficiency. Of the order of one thousand solar cell designs have been computed during the previous JPL contract [25-33] and the first year of the current contract [1,3] using this mature and exact solar cell simulator. The experience accumulated from these calculations, and their comparisons with the results published by others using other methods such as the finite difference and finite element methods, suggest that our simulator is superior and consistently gives more accurate results with negligible random noise due to truncation and discretation errors. The following is a historical summary of the use of this solar cell simulator to explore the limiting factors and barriers to higher efficiencies. It begins with the earliest simulations made in the previous contract [25] and ends with the latest simulations made in the current contract [1].

During the first application of this solar cell simulator from January 1977 to April 1978, the effects of the following factors on the solar cell efficiency were computed and studied [25]: substrate dopant impurity concentration, presence of a second and coupled recombination level or the two-electron or two-hole trap, surface recombination, and high illumination levels to 100 Suns. The steady-state local lifetimes are also displayed as a function of depth in the cell and their variation related to the fundamental capture and emission rates of carriers at the traps. Included in the displays were lifetime variations with position in the dark, at the OC (open circuit), MP (maximum power) and SC (short circuit) conditions as well as from 1 to 100

suns. The high level lifetime and high level injection conditions become very evident in the 100-sun results. Conclusions arrived at are listed as follows.

(1) Efficiency as high as 22% can be achieved for a gold recombination density of 10^{12} Au/cm³ or a base lifetime of 16 μ s. (2) The measured experimental cells doped with Ti and V are consistent with those predicted by the simulator.

(3) There is a predictable advantage of the p-based (n+/p/p+) cell over the n-based cell (p+/n/n+) due to the smaller hole lifetime in the n-base than the electron lifetime in the p-base, which advantage diminishes at the high injection level of 100 suns. (4) Higher efficiency at lower base resistivity further supports the contention that the efficiency is limited by the base lifetime or recombination in the base. (5) Increased lifetime and hence efficiency is observed in the presence of a second and coupled recombination level over the case of a one-level recombination center. (6) Impurity and defect recombination centers in the diffused emitter must have very high densities and must be physically located near the p/n junction boundary to have a significant effect in degrading the cell efficiency. For example, a lifetime of 0.1 nanosecond at the front emitter surface gives negligible efficiency reduction while it becomes significant when the recombination centers are located at the p/n junction. (7) The position, illumination level, and bias level variations of the lifetimes from the simulations indicate that experimental measurements of the lifetimes can be meaningful only if it is measured at the operating illumination and bias levels. Hence, the dark open circuit decay (DOCD) and the dark forward-injection-reverse-recovery (DFIRR) methods frequently used give substantially different lifetimes than the photoconductivity lifetimes (PCD) in strong light. It was suggested that a more reliable method than the DOCD is the small-signal illuminated open-circuit voltage decay (SSIOCD) method. Two types of small-signal excitations were

suggested: (i) a small voltage step, and (ii) a small increase or decrease of the illumination from the steady-state one AM1 sun. Another reliable method is to obtain the small-signal decay time constant of the short-circuit current transient after a small voltage step or a small illumination change. These two new methods would give lifetimes close to the OC and SC conditions. Similarly, to get the lifetimes for the maximum power condition, the current or voltage decays should be measured by biasing the cell to the maximum power condition under the desired illumination condition. To the best of our knowledge, these new methods have not been implemented by JPL and other solar cell researchers, although JPL has sponsored several subsequent lifetime measurement projects using the conventional dark methods whose resulting lifetimes are not relevant to cell performance optimization studies since they do not correspond to the OC, SC or MP conditions.

Optimization of the cell design using the solar cell simulator was continued from April 1978 to March 1979. Studies included the following [26]. (1) Back surface field substantially increases the efficiency over cells with back ohmic contacts with the major improvements in open circuit voltage from 550 mV (16.2%) without BSF to 670 mV (19.6%) with BSF and a diffused back-surface-field profile impurity density profile. (2) There is negligible difference between an ideal diffusion profile for the emitter impurity compared with an nearly abrupt profile, both giving 19.6% (19.587 versus 19.592), further supporting the contention that at 19% and above, the efficiency is mainly limited by base recombination. This conclusion eluded the solar cell researchers for the next three or four years until around 1983 when this author repeated the statement at everyone of his PIM presentations for the next three or four years that base recombination is the limit - NOT the emitter

recombination. (3) Auger recombination in the heavily doped emitter has negligible effect on the efficiency (16.236% dropped to 16.226%) and also in the heavily doped BSF layer (19.592% dropped to 19.565%). (4) Surface or interface recombination on either the front or the back surface has negligible effect on the efficiency when the emitter impurity dopant density is 10^{20} cm^{-3} . The effect becomes larger when the surface dopant density drops to 10^{18} cm^{-3} . (5) Enhanced solubility of the recombination impurity such as gold in the diffused emitter by the high density of emitter dopant impurity again has little effect on the efficiency until the substitutional gold density reaches one atomic percent, an impossible situation since it exceeds the solid solubility unless it is incorporated by ion implantation or recent superlattice technology. Even at such an improbable high concentration, the efficiency is reduced only by about 1% from 16.198% to 14.951%. The influence is less for gold in the BSF layer, for example, the efficiency drops from 19.261% without gold to 18.125% with 5% of gold in the BSF layer and assuming all 5% are electrically active recombination centers. (6) Simulation has also been made for the effect of defect-impurity pairs in the emitter and BSF layers as recombination sites on the efficiency since it is well-known that pair and higher order complexes are likely to form in the presence of high density of dopant impurities such as phosphorus and boron. Comparison was made with the Sandia high efficiency 10 ohm-cm P+/N/N+ 16.8% cell whose designed value would be 19%. It was concluded that emitter recombination with 1% gold or 0.1% boron-vacancy complex in the emitter could account for the degraded efficiency observed. (7) For the first time, the experimental silicon solar cell parameters of an impurity doped cell, in this case the Ti-doped Westinghouse cells, are compared with theory. The CTSA Solar Cell Simulator is used. Using the preliminary recombination rates of electrons and holes measured in Ti-doped junctions and crystals

(extrapolated, although very inaccurately from photoconductivity lifetime measurements), the four cell parameters computed from the simulator were in excellent agreement with the measured values, for Ti concentration from 5×10^{11} to $5 \times 10^{14} \text{ cm}^{-3}$, open circuit voltages from 550 mV to 440 mV, short circuit current density from 22 mA/cm^2 to 8 mA/cm^2 and efficiencies from 10% to 2.5%. The agreements over such a large range (three orders of magnitudes of Ti concentration) were particularly satisfying since no previous analytical theory of solar cells could be used to successfully compute their performance at such a high concentration of recombination density level that it approaches the dopant impurity concentration. At such a high density of recombination center, trapping is so high that the simple minority carrier diffusion theory is no longer valid.

A major application of the CTSA Solar Cell Simulator was its application to the determination of the allowable zinc concentration since one of the JPL material projects used zinc to reduce SiCl_4 in an fluidized bed reactor to yield low cost granular silicon. This was summarized by Lutwack on page 11 of his program report [12]. The results of this simulation was given in the third technical report of the previous contract [27] and a journal article [18]. In order to reach an efficiency of 20%, the zinc concentration in the finished cell must be less than $5 \times 10^{10} \text{ Zn/cm}^3$ in the P+/N/N+ cell and $2 \times 10^{10} \text{ Zn/cm}^3$ in the N+/P/P+ cell.

A comprehensive application of the simulator was made to determine the optimum thickness of BSF cells to achieve the highest possible efficiency since the short circuit current would decrease with decreasing thickness while the open circuit voltage will increase monotonically with decreasing thickness.

This work was reported in the fourth technical report of the previous contract [28] and published in a journal paper [32]. Only moderately efficient cells were simulated (about 16 to 17%) although the conclusion holds for higher efficiency cells. The optimum thickness was about 50 microns which is the thickness of the active base and emitter layers, not including the substrate. Thus, for manufacturability and high yields, an epitaxial layer of 50 micron thick would be the desirable starting materials. A cell optimization simulation of this type could not be accurately done using analytical solutions since both the diffusion profiles of the emitter and BSF and the nonlinear or high injection level effect in the thin base layer must be taken into account which cannot be modeled correctly by the approximate linear analytical solutions employed by many solar cell researchers.

The simulator has also been used to delineate an erroneous prediction of the thickness dependence of the fill factor by the one-dimensional low-level analytical model employed in Hovel's book on Solar Cell and by articles in Buckus's reprint collection on solar cells [29,33]. The analytical model does not predict a drop-off of the fill factor at large thickness due to neglecting the bulk series resistance and nor a rise at very small thickness when emitter recombination dominates over the base, resulting in a change from intermediate injection level in the base to low injection level in the emitter, the latter due to the high majority carrier density in the emitter. This paper illustrates one important use of the exact solution and the CTSA Solar Cell Simulator which is especially important for isolating the origin of the 1% increase or decrease of efficiency in the above 20% range. Such a delineation study would be futile using the approximate analytical theory which cannot take into account of the nonlinear carrier transport and recombination mechanisms which contribute or

are the causes.

To further improve the collection efficiency and cell performance, the simulator was employed to find the optimum parameters for a BSF cell with a built-in electric field from impurity gradient in the base. Physical intuitions indicated that the sensitivity of the efficiency to the density of the recombination impurity in the base should be substantially reduced by the presence of the built-in electric field since it helps to separate the photo-generated electrons and holes before they recombine and hence allowing higher impurity density at a prescribed efficiency. The graded base BSF structure was simulated in the first technical report of the current contract [1] and published in a journal article [2]. Using the zinc impurity as the recombination center model, it was shown that a penetration of the diffused BSF layer of 40 microns into a 50 micron based layer can give a substantial increase of the cell efficiency, from 18% to over 20%. It further shows that such a penetration or grading of the base would reduce the sensitivity to the recombination impurity density by one order of magnitude. For 20% efficiency, the Zn concentration must be less than 10^{11} Zn/cm³ in a BSF without grading. Grading increases this to 10^{12} Zn/cm³ to still maintain a 20% efficiency.

2.3 IDENTIFICATION OF EFFICIENCY LIMITING FACTORS BELOW AND ABOVE 20% AND RECOMMENDATION OF PRACTICAL SOLUTIONS (Task 3)

This objective was added to the contract about January 1, 1984 in order to focus on the new thrust in high efficiency and very high efficiency solar cell research and development undertaken by the JPL/DoE silicon solar cell program. This task contains three objectives which are: (1) identification of limiting factors below 20%, (2) quantitative analyses for high efficiency cell designs and (3) recommendation of practical solutions for greater than 20% silicon solar cells. Results of this study were reported in the second technical report [3] and an extended version was published in a special issue of the Solar Cell journal on high efficiency solar cells [4]. The invited paper [4] includes additional historical information of this DoE/JPL solar cell and other NASA solar cell programs as well as a delineation of the future research directions and needs on solar cell device and material physics and manufacturing process engineering. Since the distribution of the solar cell special issue may be delayed, this invited paper is reproduced in appendix A in its entirety.

Additional practical solutions were proposed using innovative structures which are disclosed in a NASA/JPL patent application [11]. Their disclosure in the form of a PIM report or a contract technical report has been delayed by the patent filing process. A brief summary will be given.

Investigations on the three objectives are described in the following three subsections. New results obtained or published since the release of the second technical report [2] in December, 1984, are added.

2.3.1 EFFICIENCY LIMITING FACTORS BELOW 20%

Cells with 20% or smaller efficiencies are mainly limited by carrier recombination via residual impurity and defect recombination centers in the base layer. In the highest efficiency cells reported by Green with grooved emitter surface and hence increased emitter surface recombination area, base recombination is still more than a factor of two higher than the grooved emitter whose interface recombination is almost an order of magnitude higher than the best non-grooved emitter also reported by Green. Some earlier high efficiency cells of the 17% range were also limited by the lack of a back surface field layer that shields the photo-generated electrons and holes from the back ohmic contact which has nearly infinite recombination rate.

To identify the causes which limit the cell efficiency to 20%, we compared the published cell performance data and diode dark current of selected groups of highest efficiency cells reported to date with the theory. The CTSA Solar Simulator is NOT used to give the theory for a very simple reason - in order to reach the highest efficiency, the diode must be at low injection level and follow the ideal Shockley dark diode equation, $J = J_1[\exp(qV/kT) - 1]$, which we have demonstrated [2,4], and base recombination loss must be the residual recombination loss with recombination at all other regions of the diode eliminated, which we have also demonstrated [2,4]. Thus, the ideal Shockley dark diode equation would accurately give the ultimate efficiency of a junction diode solar cell. It is most appropriate to determine how closely the experimental high efficiency cells reported to date approach that predicted by the ideal theory. This does not nullify the utility of the CTSA Solar Cell

Simulator since it is still needed to give exact simulations in order to guide the practical design of optimum cell structure or dopant concentration profile to reach the highest possible efficiency at and above 20%, for in practice, the ideal diode characteristic is difficult to attain and the CTSA Solar Cell Simulator can provide the design considerations and rules to approach the ideal diode.

To delineate the possible losses of the state-of-the-art cells, the expected performance from the ideal diode cell is tabulated in Tables I and II [2,4], and compared with those of the high efficiency cells reported to date in Table II [34-38]. The ideal diode cell performance is computed based on two input parameters: the experimentally measured J_1 and the short circuit current, J_{SC} , which is set at 36 mA from one optical pass through a cell of about 200 micron thick and an AM-1.5 illumination of 100 mW input optical power which corresponds to 32 mA at AM-1.0 of about 88.92 mW [4].

A comparison of the experimental cells with theory in Table II shows that the fill factor (FF) appears to be the remaining parameter that causes the experimental efficiency to fall below the theory. Series resistance is probably a main problem while the high base resistivity giving the nonideal or high level injection condition in the base is also a contributing factor even at 0.1 ohm-cm due to the long lifetime in the very high efficiency cells.

For all of the cells listed above, base recombination is still the main limiting loss, at least by a factor of two and often by as much as a factor of ten or higher than emitter surface recombination.

TABLE I

PERFORMANCE PARAMETERS OF THE IDEAL DIODE
 SILICON SOLAR CELLS
 (AM1 or AM1.5, 24.0C)

SOURCE	J1 (A)	JSC (mA)	VOC (mV)	FF	EFF (%)
*****	*****	*****	*****	*****	*****
THEORY	2.04E-16	36.0	840	0.8664	26.20
THEORY	2.12E-15	36.0	780	0.8588	24.12
THEORY	2.21E-14	36.0	720	0.8501	22.04
THEORY	2.30E-13	36.0	660	0.8402	19.97
THEORY	2.40E-12	36.0	600	0.8286	17.90
THEORY	2.50E-12	36.0	540	0.8151	15.85

Legned: area=1.0cm², PIN=100mW.

TABLE II

PERFORMANCE OF SEVERAL HIGH EFFICIENCY
LABORATORY SILICON SOLAR CELLS

SOURCE/AUTHORS (CELL TYPE)	J1 (A)	JSC (mA)	VOC (mV)	FF	EFF (%)	BASE R (ohm-cm)
*****	*****	*****	*****	*****	*****	*****
Green	1.8E-13		670			0.1
Green N+/P/P+	4.2E-13	38.3	661	0.824	20.9	0.2
Green N+/P/P+	2.9E-13	37.0	654	0.829	20.1	0.1
THEORY	3.2E-13	36.0	660	0.840	20.0	0.2
Green	3.2E-13	36.0	653	0.811	19.1	0.2
THEORY	6.6E-13	36.0	641	0.835	19.3	0.2
Green MINP	6.6E-13	35.5	641	0.822	18.7	0.2
THEORY	1.0E-12	36.0	628	0.834	18.9	0.15
ASEC N+/P		36.0	625	0.805	18.1	0.15
Rohatgi N+/P/P+	2.0E-12	36.0	627	0.800	18.1	0.2
THEORY	1.2E-12	36.2	627	0.834	18.9	0.3
Spitzer N+/P/P+		36.2	622	0.801	18.0	0.3
THEORY	2.0E-12	36.2	605	0.830	18.2	4.0
Rohatgi N+/P/P+	2.0E-12	36.2	605	0.786	17.2	4.0
ASEC N+/P		36.5	610	0.775	17.2	10.0

2.3.2 ANALYSIS FOR HIGH EFFICIENCY CELL DESIGNS

The reported cell performance given above has not incorporated all the possible high efficiency design considerations which have been analyzed and discussed in the literature, such as the thinner base and graded base, and further reduction of base recombination center density. The published experimental efforts have concentrated on increasing the collection area using multiple reflection by grooving or texturizing the emitter surface to increase the short circuit current. The increased emitter surface or interface area give a corresponding increase of the emitter surface recombination current which offsets the increased short circuit current. For example, without grooving, a saturation current of $1.8E-13$ A was obtained for approximately 36 mA of short circuit current. Grooving increased the short circuit current to 38.3 mA but also increased the saturation current to as high as $4.3E-13$ A so that the ratio of short circuit to saturation current, $(38.3E-3)/(0.43E-12) = 89E-9$ is actually decreased from the nongroove value of $(36E-3)/(0.18E-12) = 200E-9$. This analysis suggests that alternative methods such as reflecting back surface would be more effective since it would increase the short circuit current but not the emitter recombination area or emitter recombination current.

2.3.3 PRACTICAL SOLUTIONS FOR GREATER THAN 20% CELLS

From the foregoing analysis, it is suggested that the 20% efficiency barrier can be broken with the traditional diode cell structure with planar emitter surface by incorporating the improvements predicted by theory, such as the graded thin base [1,3], multiple back surface reflection [4,39], high/low

junction emitter [40], elimination of both perimeter [30] and bulk [31] defects, and clean processing to retain high base lifetime. Texturized and grooved front surface would only superficially increase the short circuit current since the dark current is also increased by the larger emitter interface area giving higher emitter interface recombination loss. Experimental cells incorporating these high efficiency design features are yet to be made.

Several novel techniques and cell structures were also suggested which could improve the efficiency and ease the critical processing requirements to break the 20% barrier. Among the novel techniques is the use of polysilicon emitter thin stripes to reduce the emitter surface recombination loss at the dark contact stripe diodes [2,4]. Based on the data of Neugroschel [41], whose recombination velocity measurements of polysilicon emitter contacts gave values less than 112 cm/sec, and a five percent stripe area, the dark current density is 2.15×10^{-14} A/cm² if base recombination is eliminated. This would give an open circuit voltage of 720 mV and 22% AM1 efficiency as indicated in Table I.

An novel structure approach was also suggested using a two-junction three-layer bipolar transistor structure with a non-contacting floating emitter [11]. This structure makes use of the bipolar transistor action in contrast to the multijunction layer tandem junction cells which connects noninteracting diodes in series. The first researchers from Texas Instruments called it the tandem junction cell, a name which we discard, since it does not reflect the bipolar operation principle. The contacts to the cell are made to the base and the collector layers. The emitter recombination loss at the dark emitter contact diode is completely eliminated since there is no emitter contact, in addition, the lateral series resistance loss in the thin high resistance

emitter layer is also eliminated since there is no emitter current. The fill factor should approach the ideal diode value. Since the collector junction also gives rise to a photocurrent generator, the short-circuit current should also increase over that of a diode solar cell which has only one junction. The main limiting factor of a two-junction three-layer bipolar transistor solar cell is the lateral base resistance which must be minimized. Known experiences in designing high efficiency bipolar power transistors could be used.

2.4 EXPERIMENTAL DEMONSTRATION AND PRACTICAL IMPLEMENTATION

This phase of the project was undertaken by another contractor and there was also plan to fabricate cells in-house following the high-efficiency design principles. The progresses would presumably be reported in the future under other continuing programs on high efficiency solar cell research.

III. CONCLUSION

The exact computer simulator adapted to solar cell efficiency maximization and applied to nearly one thousand cell design studies has proved to be an extremely powerful tool to provide accurate optimization of device parameters and geometries. This CTSA Solar Cell Simulator is useful not only for lower efficiency recombination-impurity-doped cells to ascertain the effects of impurities but also indispensable for optimization of material properties to achieve maximum efficiency exceeding 20%. For the high efficiency cells, the reason for the need of an exact simulator is the interaction among the base and emitter doping concentration and their depth profile and the injection level which controls the last drop of the fill factor. This one-dimensional simulator, although has no equals, needs to be extended to two dimensions which would require the use of a supercomputer to run. For one-dimensional simulations with 200 grid points or layers, 60 CPU seconds on a CDC-CYBER-175 (approximate speed is about 5 Mips) are required. A 200x200 two-dimensional grid would give too long a turn around time to allow for effective real-time design optimization. On a CRAY, the turn-around time would be about the same, 60 s, for a two-dimensional simulation which would be a reasonable turn-around time for studying optimum grid size and placement as well as dopant impurity profiles. The development of the two-dimensional CTSA simulator has been planned since 1977 and its implementation will be realized in FY86 or FY87 due to the availability of a CRAY-II in Urbana.

With the advances in the solar cell technology in the past 10 years under JPL management and elsewhere and JPL's redirection to focus on very high efficiency cells to exceeding the 20% barrier, the sophistication in the design

theory of solar cell, required to accurately predict cell performance, has drastically reduced and turned around a 360 degree circle. It started with the ideal diode theory in the 1950s used by M. B. Prince [4] which was the only theory available. It then migrated from the exact theory, such as the CTSA Solar Cell numerical Simulator developed at the beginning of this 10-year research project for low efficiency cells, back again to the ideal analytical theory of the Shockley diode in the last few years for research on the very high efficiency cells. This backward migration of the sophistication of the mathematical modeling of the solar cell is dictated by the low injection level requirement to break the 20% barrier and this low injection level condition is precisely the basis of the Shockley ideal diode law.

There are many traditional and recently developed design criteria which must be implemented in an experimental diode-type cell to reach the theoretically predicted efficiency of more than 20%. Some of these are thin and graded base in a back-surface-field structure, careful elimination of perimeter recombination and shorts across the back-surface-field junction as well as the front surface p/n junction, incorporation of the high/low junction in the emitter to shield the photo-generated electrons and holes from the emitter surface or interface recombination centers, poly-silicon emitter contact barriers to reduce recombination from the dark contact diode, and further improvement of base lifetime which may become less critical using the graded base just stated. All of these are suggested and described in this report. Implement of all of these high efficiency designs in one single cell has not been reported. It is believed that combination of these high-efficiency device design with careful and high-life processing would produce cells exceeding 20% efficiency without using artificial concentration schemes such as the

texturized or grooved front surface. Further improvement of efficiency may be made using back surface optical reflection to increase the absorption and hence the short circuit current. A reflecting back surface is preferred over the texturized or grooved front surface since the interface recombination current is proportional to the front surface area.

To significantly exceed the 20% barrier and to reach the intrinsic efficiency of about 25%, all of the emitter recombination losses must be eliminated and the residual losses would all come from the intrinsic (interband thermal recombination and interband Auger recombination) recombination losses in the base. For such a cell, the high-efficiency design rules need to be supplemented by innovative or novel device structures. One of this is the floating emitter two-junction bipolar transistor solar cell structure. A number of floating emitter structures are proposed as a result of the study made in this program. The epitaxial front contact floating emitter cell appears to be the most fabricable and manufacturable structure.

To reach the intrinsic efficiency of 25.5%, exceptionally clean and stress-free fabrication processes must be employed and growth techniques of very long lifetime single crystalline silicon (about one millisecond) must be developed. For the two-junction floating emitter cell, long lifetime epitaxial growth technique for 50 micron thick films must be developed. These requirements exceed the current best state-of-the-art silicon integrated circuit research and production technology and must be developed for junction areas of more than four or five inch diameter.

The severe demand on crystal and device purity and perfection from the

very high efficiency requirement eliminates all other alternative forms of materials, such as polycrystalline cells, amorphous film cells and other yet to be invented novel material compositions, as viable candidates for the very high efficiency solar cells. This conclusion holds not only for very high efficiency crystalline silicon cells but also cells made on other materials and cells having multiple junctions either in tandem diode or in bipolar transistor forms. Manufacturing cost will be the ultimate deciding factor on whether the very high efficiency crystalline solar cell or lower efficiency cells on polycrystalline or amorphous materials is the economically viable choice for terrestrial applications.

IV. REFERENCES

- [1] C. T. Sah, "Study of relationships of material properties and high efficiency solar cell performance on material composition," First Technical Report, DOE/JPL-956289-83/1, July 1983.
- [2] C. T. Sah, "High efficiency crystalline silicon solar cells," Second Technical Report, DOE/JPL-956289-84/1, December 1984.
- [3] C. T. Sah and F. A. Lindholm, "Performance improvements from penetrating back-surface field in very high efficiency terrestrial thin-film crystalline silicon solar cell," Journal of Applied Physics, v55(4), pp. 1174-1182, 15 February 1984, and F. A. Lindholm and C. T. Sah, "Theoretical performance limits and measured performance of thin extended back-surface-field p/n junction silicon solar cells," Proceeding of 1984 International Photovoltaic Specialist Conference, pp.1202-1206, IEEE Publication Catalog CH2019-9/84.
- [4] C. T. Sah, "High efficiency crystalline silicon solar cells," Solar Cells special issue, invited paper, March 1986. See also Appendix A.
- [5] C. Tang Sah, "Parameters affecting the performance of high efficiency silicon solar cells," Proceeding of the High-Efficiency Solar Cell Modeling Workshop, March 13, 1984, Jet Propulsion Laboratory, and "Barriers to achieving high efficiency," Proceedings of the 23rd Project Integration Meeting held on March 14-15, 1984. PROGRESS REPORT 23, Jet Propulsion Laboratory, pp.123-120, JPL Publication No. 84-47.
- [6] C. Tang Sah, "Recombination phenomena in high efficiency silicon solar cells," Proceedings of the Flat-Plate Solar Array Project Research Forum on High-Efficiency Crystalline Silicon Solar Cells Research Forum, July 9-11, 1984, Phoenix, AZ, Jet Propulsion Laboratory Publication No. 5101-258 (DOE/JPL-1012-103) pp. 37-51, May 15, 1985.
- [7] C. Tang Sah, "Important loss mechanisms in high efficiency solar cells," Proceeding of the 24th Project Integration Meeting held on October 2-3, 1984 and PROGRESS REPORT 24, Jet Propulsion Laboratory Report No. 5101-259 (DOE/JPL-1012-104), pp.347-351, distributed June, 1985.
- [8] C. Tang Sah, "Study of material properties and high efficiency solar cell performance on material composition," Proceedings of the 25th Project Integration Meeting held on June 19-20, 1985 and PROGRESS REPORT 25, Jet Propulsion Laboratory Publication No. 5101-??? (DOE/JPL-1012-???), pp.xxx-xxx, distributed June, 1986.
- [9] C. Tang Sah, "High efficiency solar cell," Proceedings of the 26th Project Integration Meeting held on April 29-30, 1986 and PROGRESS REPORT 26, Jet Propulsion Laboratory Publication No. 5101-???.
- [10] C. Tang Sah, "Requirements for high-efficiency solar cells," Proceedings of Flat-Plate Solar Array Workshop on Low-Cost Polysilicon for Terrestrial Photovoltaic Solar Cell Applications held on October 28-30, 1985, Las Vegas, xx-xx, Jet Propulsion Laboratory Publication No. ?.

- [11] Chih Tang Sah and Li-Jen Cheng, "Floating emitter solar cell junction transistor," JPL Case No. 16467 and NASA Case No. NPO-16467-1-CU.
- [12] Ralph Lutwack, "A review of the silicon material task," Jet Propulsion Laboratory Publication 5101-244 (DOE/JPL-1012-96), 34 pages, February 1, 1984.
- [13] J. R. Davis, A. Rohatgi, R. H. Hopkins, P. D. Blais, R. Rai-Choudhury, J. R. McCormick and H. C. Mollenkoph, "Impurities in silicon solar cells," IEEE Trans. Electron Devices, ED-27, 677 (1980).
- [14] K. A. Yamakawa, "The effects of impurities on the performance of silicon solar cells," Jet Propulsion Laboratory Publication 5101-189 (DOE/JPL-1012-57), 80 pages, September 1, 1981.
- [15] J. M. Blocher, Jr. and M. F. Browning, "Evaluation of selected chemical processes for production of low-cost silicon," Phases I and II Final Report, DOE/JPL 954339-78/11, July 9, 1978; Quarterly Reports, DOE/JPL 954339-79/15, August 15, 1979, DOE/JPL 954339-80/20, December 19, 1980; BATTELLE Columbus Laboratories, 505 King Avenue, Columbus, OH 43201.
- [16] C. T. Sah, L. Forbes, L. L. Rosier and A. F. Tasch, Jr., "Thermal and optical emission and capture rates and cross sections of electrons and holes at imperfection centers in semiconductor from photo and dark junction current and capacitance experiments," Solid-State Electronics, v13(6), pp.759-788, June 1980; C. T. Sah, "Detection of recombination centers in solar cells from junction capacitance transients," IEEE Trans. Electron Devices, ED-24(4), pp.410-419, April 1977. For a summary of our earlier work, see C. T. Sah, "Bulk and interface imperfections in semiconductors," Solid-State Electronics, 19(12), 975-990, December 1976; and C. T. Sah, "Detection of defect and impurity centers in semiconductors by steady-state and transient junction capacitance and current techniques," Semiconductor Silicon-1977, Proceedings of the Third International Symposium on Silicon Materials Science and Technology, v77-2, 868-893, May 9-13, 1977.
- [17] Alex C. Wang and C. T. Sah, "New method for complete electrical characterization of recombination properties of traps in semiconductors," J. Applied Physics, 57(10), 4645-4656, 15 May 1985.
- [18] C. T. Sah, Phillip C-H Chan, C-K Wang, Robert L-Y Sah, K. Alan Yamakawa, and Ralph Lutwack, "Effect of zinc impurity on silicon solar-cell efficiency," IEEE Trans. Electron Devices, ED-28(3), 304-313, March 1981.
- [19] Alex C. Wang and C. T. Sah, "Determination of trapped charges emission rates from nonexponential capacitance transients due to high trap densities in semiconductors," J. Appl. Phys. 55(2), 565-570, January 15, 1984.
- [20] Alex C. Wang and C. T. Sah, "Electron capture at the two acceptor levels of zinc center in silicon," Phys. Rev. B, 30(10), 5896-5903, November 15, 1984.
- [21] Alex C. Wang and C. T. Sah, "Complete electrical characterization of

- recombination properties of titanium in silicon," J. Appl. Phys. 56(4), 1021-1031, August 15, 1984.
- [22] Luke Su Lu and C. T. Sah, "Effects of surface recombination and channel on the Capacitance Transient Spectroscopy," to be published.
- [23] Luke Su Lu and C. T. Sah, "Electron recombination rates at the gold acceptor level in high-resistivity silicon," J. Appl. Phys. 59(1), 173-178, 1 January 1986.
- [24] Henry Brandhorst as quoted in R. R. Ferber, E. N. Costgoue and K. Shimada, "Multijunction cells for concentrators: technology prospects, Issue Study," Jet Propulsion Laboratory Report DOE/ET/20356-18 (DE85006659), November 15, 1984. Statement of Brandhorst on lines 28-40, page 6.
- [25] C. T. Sah, "Study of the effects of impurities on the properties of silicon materials and performance of silicon solar cells," April 1980, Technical Report No. 1, DOE/JPL-954685-78/1, Jet Propulsion Laboratory.
- [26] ibd. March 1979. Technical Report No. 2, DOE/JPL-954685-79/1.
- [27] ibd. February 1980. Technical Report No. 3, DOE/JPL-954685-80/1.
- [28] ibd. March 1981. Technical Report No. 4, DOE/JPL-954685-81/1.
- [29] ibd. October 1981. Technical Report No. 5, DOE/JPL-954685-81/2.
- [30] C. T. Sah, K. A. Yamakawa and R. Lutwack, "Reduction of solar cell efficiency by edge defects across the back-surface-field junction: - a developed perimeter model," Solid-State Electronics, 25(9), 851-858, September 1982.
- [31] C. T. Sah, K. A. Yamakawa and R. Lutwack, "Reduction of solar cell efficiency by bulk defects across the back-surface-field junction," J. Appl. Phys. 53(4), 3278-3290, April 1982.
- [32] C. T. Sah, K. A. Yamakawa and R. Lutwack, "Effect of thickness on silicon solar cell efficiency," IEEE Trans. Electron Devices, ED-29(5), 903-908, May 1982.
- [33] C. T. Sah, "Thickness dependences of solar cell performance," Solid-State Electronics, 25(9), 960-962, September 1982.
- [34] Joseph B. Milstein and Y. Simmon Tsuo, "Research on crystalline silicon solar cells," Conference Record of the 17-th IEEE International Photo-voltaic Specialists Conference, May 1-4, pp. 248-251, IEEE Catalog No. CH2019-8/84, IEEE 445 Hoes Lane, Piscataway, NJ 08854.
- [35] J. B. Milstein and C. R. Osterwald, "High efficiency solar cell program: some recent results," Proceedings of the 23rd Project Integration Meeting held on March 14-15, 1984, PROGRESS REPORT 23, Jet Propulsion Laboratory Publication No. 84-47, pp.151-157 (DOE/JPL-1012-99); J. B. Milstein, "Rapid advances reported in silicon solar cell efficiency," IN REVIEW (A SERI Research Update), Vol. VI(3), p.5, March 1984, Solar Energy

Research Institute, Golden, CO.

- [36] A. W. Blakers and M. A. Green, "20% efficiency silicon solar cells," Appl. Phys. Lett. 48(3), 215-217, 20 January 1986. Martin A. Green, A. W. Blakers, J. Shi, E. M. Keller and S. R. Wenhan, "High-efficiency silicon solar cells," IEEE Trans. ED-31(5), 679-683, May 1984.
- [37] Mark B. Spitzer, S. P. Tobin, C. J. Keavney, "High-efficiency ion-implanted silicon solar cells," IEEE Trans. ED-31(5), 546-550, May 1984.
- [38] Ajeet Rohatgi and P. Rai-Choudhury, "Design, fabrication and analysis of 17-18 percent efficient surface-passivated silicon solar cells," IEEE Trans. ED-31(5), 595-601, May 1984; Ajeet Rohatgi, "Process and design considerations for high-efficiency solar cells," Proceedings of the Flat-Plate Solar Array Project Research Forum on High-Efficiency Crystalline Silicon Solar Cells July 9-11, 1984, pp.429-446, JPL Publication 85-38, (DOE/JPL-1012-103), May 15, 1985.
- [39] C. T. Sah, "Prospects of amorphous silicon solar cells," Jet Propulsion Laboratory Document No. DOE/JPL-660411-78/01, 87 pages, 31 July 1978.
- [40] C. T. Sah, F. A. Lindholm and J. G. Fossum, "A high-low junction emitter structure for improving silicon solar cell efficiency," IEEE Trans. on Electron Devices, ED-25(1), 66-67, January 1978.
- [41] A. Neugroschel, M. Arienzo, Y. Komen and R. D. Issac, "Experimental study of the minority-carrier transport at the polysilicon-monosilicon interface," IEEE Trans. Electron Devices, ED-32(4), 807-816, April 1985. See also Arnost Neugroschel, presented by C. T. Sah at the 24th Project Integration Meeting, October 2-3, 1984, PROGRESS REPORT 24, pp.283-294, Jet Propulsion Laboratory Publication 85-27 (DOC/JPL-1012-104).

APPENDIX

HIGH EFFICIENCY CRYSTALLINE SILICON SOLAR CELLS

44 pages.

This is reference [4] cited in the main text of this final report. It has been scheduled for publication as an invited paper in the special issue of the journal, SOLAR CELLS, for February, 1986. It is included here as an appendix in its entirety for ease of reference in view of the publication delay of this special Solar Cell journal issue.

HIGH EFFICIENCY CRYSTALLINE SILICON SOLAR CELLS

C. T. Sah

Department of Electrical and Computer Engineering

University of Illinois

Urbana, Illinois 61801

ABSTRACT

Base recombination at residual defect and impurity recombination centers are identified to be the likely cause of the 20% (AM1) efficiency barrier in the highest efficiency silicon solar cells reported to-date. To reach the 20%-AM1 efficiency, base recombination must be further reduced by either stress-free and clean fabrication techniques on high lifetime crystals or novel base structure design, such as the graded thin-base back-surface-field structure proposed and analyzed by Sah and Lindholm. To break the 20% barrier, residual base recombination losses must be eliminated and emitter recombination must be reduced. Several novel emitter designs to reduce recombination losses have been proposed and one demonstrated. These involve the reduction of emitter interface recombination losses at the non-contact surface by high quality thermal oxide and at metal-contact/silicon-emitter interface by either a thin tunneling oxide, as demonstrated by Green, or by a polysilicon barrier layer between the metal conductor and the silicon emitter surface. Efficiency of 23.8%-AM1 has been estimated using Neugroschel's data of emitter interface recombination velocity and dark current density of polysilicon barrier layers. Novel floating emitter or non-contact emitter solar cell transistor structures have also been proposed by Sah and Cheng to reduce emitter recombination loss for beyond-20% efficiency silicon solar cells.

I. INTRODUCTION

The photovoltaic phenomenon was discovered by Becquerel in 1839 who observed a light induced voltage when one of electrodes in an electrolyte was exposed to light [1]. The term cell used in solar and other photovoltaic cells was probably first introduced by Bidwell in 1885 [2]. The first solar cell in silicon p/n junction was demonstrated by Chapin, Fuller and Pearson at the Bell Laboratories in 1954 [3] who reported an efficiency of 6%. Photovoltaic effect at rectifying contacts to Cadmium Sulfide single crystals was also observed in 1954 by Reynolds, Leies, Antes and Marburger at the U. S. Air Force Aerospace Research Laboratory [4]. Since then, substantial progresses have been made towards the development and application of p/n junction solar cells for power generation. The most successful and extensive applications have been in providing power for satellites in space. A focused development effort for low cost terrestrial photovoltaic power generation systems was suggested in the earlier 1970's [5,6] and began in earnest when in 1972 the Ad Hoc Panel on Solar Cell Efficiency of the National Academy of Science - National Research Council recommended that a national research and development program be initiated to increase the silicon solar efficiency to 20% [7]. A ten year program was proposed by the Rappaport Single-Crystal Silicon Solar Cell Workshop Group in 1973 [8] with a 1985 goal of 20% AM1 efficiency and \$0.50 per peak kilowatt in 1973 dollar. A comprehensive biography of solar cell literature up to 1974 was compiled by Backus whose edited volume also contains reprints of selected papers of historical significance [9]. A historical review up to 1972 was given by Wolf [9].

II. RECENT DEVELOPMENTS

Based on the NAS-NRC and NSF panel recommendations, a focused ten-year program began in 1975 with the Jet Propulsion Laboratory of U.S. National Aeronautics and Space Administration as the program manager for the U. S. Department of Energy. Its principal mission was to develop the technology to produce low-cost solar array for terrestrial applications. This paper gives a review, from the author's perspectives, of the focus on the silicon p/n junction solar cell physics for improving efficiency, from the inception of this program to the latest state-of-the-art. It also gives a projection of the research and development needs to reach the intrinsic performance limits. To-date, most of the goals laid down by the Rappaport Group [8] are nearly reached. Further developments, all in silicon device process technology, as originally anticipated by the NAS-NRC panel [7], must be undertaken to exceed the 20%-AM1 barrier.

The remaining sections of this article are based on a contract report prepared by the author [10]. The third section will provide an analysis of the factors which may limit the cell efficiency to below 20%. An evaluation is also given of the factors which limit the efficiency to less than 20% in the state-of-the-art crystalline silicon solar cells reported in the literature. The fourth section will summarize the analysis to give cells with greater-than-20% efficiency. Suggestions for practical designs of high efficiency cells with greater than 20% efficiency are made in section five. Conclusion and summary are given in section VI.

III. LIMITING FACTORS BELOW 20% (AM1)

In order to delineate the factors which limit the silicon solar cell performance below or above 20% AM1 efficiency, a general analysis of the electrical characteristics is first given, in section 3.1. The various recombination loss mechanisms and their locations in the solar cell structure are then identified, elucidated and estimated in section 3.2. The limiting recombination loss mechanisms and sites in the highest efficiency silicon solar cells reported in the literature are then delineated in section 3.3.

3.1 GENERAL DESCRIPTION OF THE SOLAR CELL CURRENT-VOLTAGE CHARACTERISTICS

The performance of solar cells has been estimated, predicted and computed from the solution of the six semiconductor equations by various techniques and approximations. These six equations, also known as the Shockley Equations, are given below for the d.c. steady-state condition.

$$\vec{J}_N = + qD_n \nabla N + q\mu_n N \vec{E} = - q\mu_n N \nabla V_N \quad (3.1.1)$$

$$\vec{J}_P = - qD_p \nabla P + q\mu_p P \vec{E} = - q\mu_p P \nabla V_P \quad (3.1.2)$$

$$0 = + \nabla \cdot \vec{J}_N - I_N \quad (3.1.3)$$

$$0 = - \nabla \cdot \vec{J}_P + I_P \quad (3.1.4)$$

$$\nabla \cdot (\epsilon \vec{E}) = \rho = q(P - N + N_{DD} - N_{AA} - N_T) = - \nabla \cdot (\epsilon \nabla V_I) \quad (3.1.5)$$

$$0 = + I_P + I_N \quad (3.1.6)$$

The first two equations are the electron and hole areal current density equations whose components are the diffusion currents with diffusivities D_n and D_p and the drift currents with mobilities μ_n and μ_p for electrons and holes respectively. The volume density or concentration of the electrons and holes are given by N and P respectively while \vec{E} is the electric field vector and q is the magnitude of the electron charge.

The second two equations are the current continuity equations which state that the divergence of the electron or hole current density is given by the net volume current generator or source, I_N or I_P respectively. Due to the establishment of d.c. steady-state, these two current sources are equal in magnitude and opposite in sign as indicated by the sixth equation, (3.1.6), given above.

The fifth equation is the Poisson equation which relates the divergence of the electrical displacement, $\epsilon \vec{E}$, to the net macroscopic volume space charge density, ρ . The latter consists of the contributions of the holes in the valence band, the electrons in the conduction band, the ionized donors, N_{DD} , the ionized acceptors, N_{AA} , and the charges trapped at the recombination centers, N_T .

The sixth equation is derived from the general kinetic or time-dependent rate equation of recombination of electrons and holes. It is the most important equation in device physics. However, it has been incorrectly treated by many device theorists even to this day. The general time dependent form is given by

$$q(\partial n_T / \partial t) = i_N + i_P \quad (3.1.7)$$

where n_T is the time dependent form of the trapped electron density at the recombination centers which can be decomposed into a d.c. steady-state component and time-vary component, $n_T(\vec{r}, t) = N_T(\vec{r}) + n_t(\vec{r}, t)$. At d.c. steady state, $\partial n_T / \partial t = 0$, so that

$$I_P = -I_N = I_{SS} \quad (3.1.8)$$

where I_{SS} is the net steady-state volume generation current density from all the electron-hole generation-recombination mechanisms. It is these mechanisms that produce the photocurrent and photopower by a solar cell. It is also these mechanisms which limit the solar cell power conversion efficiency to less than 100%.

For solar cells with an one-energy-level recombination center and exposed to solar illumination, I_{SS} is composed of a optical generation component and a recombination component. The recombination component can consist of as many as nine parts each from a different recombination mechanism to be discussed in the next subsection.

There have been many extensive efforts to solve these six equations numerically on high speed computers. The exact one-dimensional code has been completely developed, debugged and used for many solar cell design runs since 1978 [11]. Many cell-design calculations have been reported in JPL technical reports [11-16] and journal articles [16-21]. This code is based on the circuit technique for semiconductor analysis [22] and is considered mature. It can give the current-voltage and internal characteristics of solar cells with any dopant and recombination impurity profiles, including interface and surface recombination centers, and as many as two recombination energy levels, from two independent recombination center species or from one species of two-level recombination centers, such as Ti, Zn, S, Au, V and others.

Other efforts of providing codes for numerical solutions of the six semiconductor equations have been less successful as suggested by the lack of published report of cell designs. Most of the other efforts have also included some approximations to the six equations prior to numerical solution. The most serious one which is wide spread is the exclusion of the sixth equation. These authors also neglected the charge trapped at the recombination centers, $N_T(\vec{r})$, in the fifth or Poisson equation. There is no assurance that an accurate solution can be obtained when the trapped charge term is dropped, although it may be much smaller than the dopant charge density terms, N_{DD} and N_{AA} . Its importance even at 10^{10} cm^{-3} level has been demonstrated by us [23-24].

Another approach to the solution of the solar cell current-voltage characteristics is to develop an analytical and hence approximate solution from the six semiconductor equations. The most famous and widely used one is that of the ideal diode law first given by Shockley in 1949 which was first used by Prince [25] in 1955 in an extensive analysis of the performance of p/n junction solar cells with practical geometries. This dark current-voltage equation for an ideal diode can be readily extended to give us a generalized and simple solar cell equation which can serve as a guide for the delineation of the various recombination loss mechanisms in very high efficiency solar cells. The following is a sketch of the derivation of this analytical approximation. It provides a ball-park estimate of the critical values of the recombination parameters for cells below and above 20% AM1 efficiency.

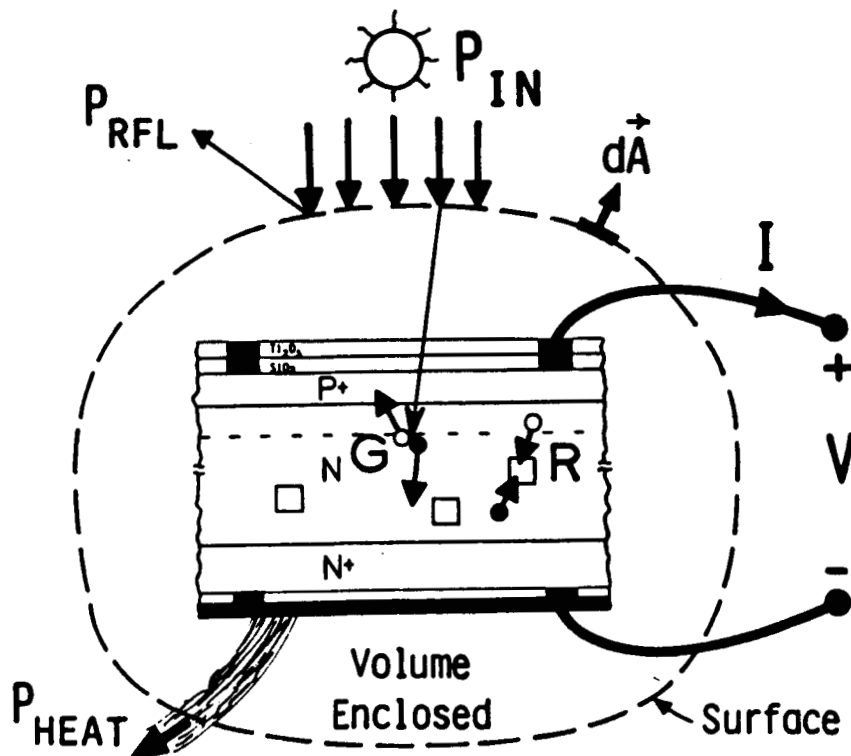


Fig. 1 A cross-section view of a solar cell for the derivation of the general solar cell current-voltage equation.

With reference to a general solar cell structure shown in Fig.1, we may apply the three-dimensional continuity equations given by Eqs. (3.1.3) or (3.1.4) by integrating it over a surface which encloses the entire cell as illustrated in Fig.1. We decompose the net volume generation current density, I_{SS} , into its two components explicitly, $I_{SS}=q(G-R)$, where G is the optical generation current density inside the cell due to the penetrated solar illumination and R is the net recombination current density, in all parts of the cell including the bulk, interface as well as surface. Then, using the divergence theorem to transform the volume integral of $\nabla \cdot \vec{J}_P$ or $\nabla \cdot \vec{J}_N$ into a surface integral, we get

$$\oint \nabla \cdot \vec{J}_P dV = \oint \vec{J}_P \cdot d\vec{A} = I = q \oint (G-R)dV = I_L - I_R \quad (3.1.9)$$

Here, I_L is the photocurrent generator and I_R is the diode current-voltage characteristics. In the case of a linear system, where the recombination law is linear in the electron and hole concentrations, then I_R is just the dark diode current-voltage characteristics given by Sah [26].

$$I_R = \sum_{m=1}^4 J_m A_m [\exp(qV/mkT) - 1] \quad (3.1.10)$$

where the sum is taken over the various recombination regions and $m=1$ to 4 as summarized below and elaborated in the next subsection.

m-Value	RECOMBINATION REGIONS
*****	*****
1	Quasi-neutral base and emitter layers.
1	Front and back surfaces or interfaces.
1 to 2	High level condition in above regions.
1 to 2	Space charge layer.
2 to 4	Surface channel.

An indication can be made of the requirement on the recombination current density coefficient, J_m given in Eq.(3.1.10), to achieve high performance. For this purpose, the best case is taken, namely that of $m=1$ since this gives a

current-voltage characteristics which is closest to the ideal lossless case of a square (or rectangular) I-V curve sometimes known as the threshold case. Figure 2 illustrates the IV characteristics of these cases.

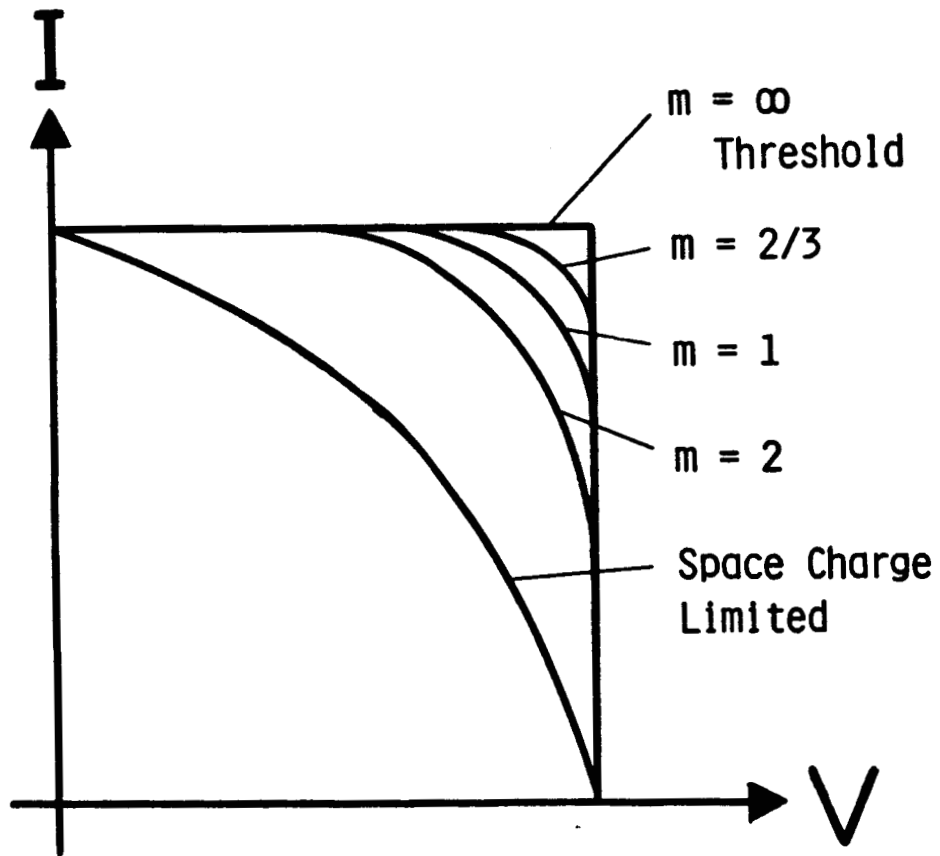


Figure 2 The current-voltage (IV) characteristics of several p/n junction solar cells with different recombination loss mechanisms.

For general comparisons, we also assume that illuminated area is equal to the cross-sectional area of the recombination volume. Thus, the ideal (but not lossless) solar cell characteristics can then be described by

$$J = J_L - J_1[\exp(qV/kT) - 1] \quad (3.1.11)$$

where J is the current density flowing into the external circuit from the solar cell power source and V is the terminal voltage of the cell. We have neglected the internal series resistance losses of the cell in this ideal case.

The photocurrent density is a weak function of recombination loss in high efficiency cells. It can be taken as a constant and set to the maximum available photocurrent under AM1 illumination at a given cell thickness. Our example here and in the remaining sections of this report will take a value of 36 mA/cm^2 for J_L which corresponds to the laboratory simulated solar power density at the earth surface, known as AM1.5, at a photopower density of $\text{PIN} = 100 \text{ mW/cm}^2$. This closely approximates the photocurrent generated in a 50 micron thick photoactive layer of a cell, with no front and back surface reflection, and under the real AM1 solar spectral density of 88.92 mW/cm^2 which gives a photocurrent of 31.49 mA/cm^2 obtained by a numerical solution of the six semiconductor equations using the circuit techniques. (See Table III of reference [17].) This gives a photocurrent response of $J_{SC}/\text{PIN} = 31.49/88.92 = 0.3541 \approx 0.36 \text{ A/W}$. For other illumination intensities, material properties and cell thickness, only the ratio, $J_L/\text{PIN} = 36/100 = 0.36 \text{ A/W}$, needs to be modified and the results can be scaled. For example, if the cell was infinitely thick or all photons were absorbed, then this photo-response ratio is increased by 27.6% to 0.4594 A/W . Infinitely thick cell is neither practical nor desirable since the neglected series ohmic loss will be increasingly important to reduce the efficiency. Multiple-pass in thin cells would be a solution to increasing the photocurrent while keeping the series resistance loss low. The

two-pass case with perfect reflecting back surface has been analyzed by us [20] which showed marginal improvement. Figure 3 gives the available photocurrent for the front and back surface illuminated silicon cells as a function of thickness under AM0 and AM1 (88.92mW) illumination conditions [27]. The sum of the available photocurrents from the front and back illuminated one-pass cell is the upper limit of the two-pass cell with perfect back surface reflection. It is evident that only when the cell is very thin can the back surface reflection improve the short-circuit current significantly.

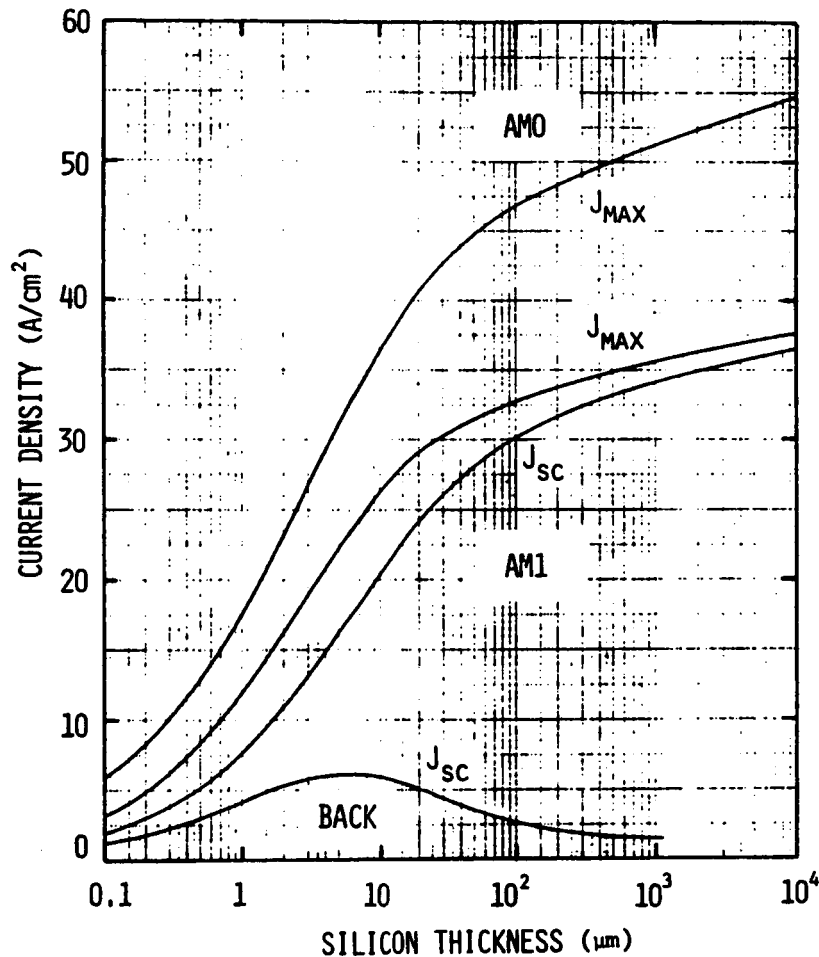


Figure 3 The available photocurrent or maximum short-circuit current in silicon solar cells as a function of silicon thickness under AM0 and AM1 (88.92 mW) illumination conditions for one-pass front or back illuminated cells.

The performance of the solar cell is characterized by four parameters, the short-circuit current, J_{SC} , the open-circuit voltage, V_{OC} , the efficiency at the maximum load power point, EFF , and the fill factor (sometimes also known as the curve factor or form factor) at the maximum load power point, FF . These can be computed from Eq.(3.1.11) and are given by

$$J_{SC} = J_L = J_1 * [\exp(q * V_{OC} / kT) - 1] \quad (3.1.12)$$

$$EFF = P_{MAX} / P_{IN} = J_{MAX} * V_{MAX} / P_{IN} \quad (3.1.13)$$

$$FF = J_{MAX} * V_{MAX} / J_{SC} * V_{OC} \quad (3.1.14)$$

where the maximum load power point is obtained by setting the derivative $dP/dV = d(J * V) / dV$ to zero using Eq.(3.1.11) for J . The maximum efficiency can also be computed from

$$EFF = FF * J_{SC} * V_{OC} / P_{IN} = (J_{SC} / P_{IN}) * FF * V_{OC} = 0.36 * FF * V_{OC} \quad (3.1.15)$$

in this case. FORTRAN notation convention is used here.

The results given by Eqs.(3.1.12) to (3.1.15) are particularly useful to provide a guide in the search of solar cell geometries of high efficiency. To illustrate the numerical range of the parameters in high efficiency cells, a set of parameters are computed and tabulated in Table I. It shows that the dark current, J_1 , must be less than $2.3E-13$ A/cm² or 0.2 pA/cm² for a 20%-AM1 cell. It decreases about one decade for each efficiency rise of 2%, reducing to 0.2 fA/cm² at about 26%, which is about the ultimate intrinsic limit for a silicon solar cell with 50 microns of photoactive layer as indicated in section 4. The table also shows that for each 2% rise of efficiency, the open-circuit voltage must increase by about 60 mV, consistent with a simple estimate of 58.96 mV or $2.303kT/q$.

TABLE I
 PERFORMANCE PARAMETERS OF THE IDEAL DIODE
 SILICON SOLAR CELLS
 (AM1 or AM1.5, 24.0C)

SOURCE	J1 (A)	JSC (mA)	VOC (mV)	FF	EFF (%)
*****	*****	*****	*****	*****	*****
THEORY	2.04E-16	36.0	840	0.8664	26.20
THEORY	2.12E-15	36.0	780	0.8588	24.12
THEORY	2.21E-14	36.0	720	0.8501	22.04
THEORY	2.30E-13	36.0	660	0.8402	19.97
THEORY	2.40E-12	36.0	600	0.8286	17.90
THEORY	2.50E-11	36.0	540	0.8151	15.85

Legend: Area=1.0cm², PIN=100mW.

The numerical results of Table I also shows the range of the dark current density, J1, for the less-than 20% cells. For these cells, the dark current is more than 0.23 pA/cm² if the losses are all in the quasi-neutral regions and layers or at the interfaces and the cells are at a low injection level so that they follow the ideal diode law. In general, cells with lower efficiencies suffer also from recombination losses at the resistive defects or short circuit spots on the cell perimeters [18] and in the bulk and back contact regions [19], in the surface channels [26] as well as at recombination centers in the quasi-neutral base layer, the last from residual crystal growth- and process-induced metallic recombination impurities.

3.2 RECOMBINATION LOSS MECHANISMS AND SITES

Energy loss by photogenerated electrons and holes through scattering and recombination limits the ultimate performance of solar cells. Scattering reduces the mobilities of electrons and holes, increases the series resistance and decreases the fill factor measured externally. Recombination losses increase the shunt conductance and the dark leakage current which decrease both the open-circuit voltage and the short-circuit current. Energy losses of the photogenerated electrons and holes by these two collision processes, scattering and recombination, will thereby reduce the efficiency of the solar cell since it is given by the product of the open-circuit voltage and the short-circuit current as indicated by Eq.3.1.13.

3.2.1 CLASSIFICATION OF RECOMBINATION PROCESSES

The electron-hole recombination processes can be categorized according to their origin and further delineated by the energy exchange mechanisms which control the recombination rate. Recombination processes with the intrinsic origin are those which limit the ultimate performance of a solar cell. Recombination processes with the extrinsic origin due to crystal imperfections, such as chemical impurities and physical defects present in the electrically active volumes of the cell, is the dominant reason that limited the best silicon solar cell to-date to an efficiency below 20%-AM1. However, the extrinsic origin of the recombination losses can obviously be reduced with advanced and by future advances in silicon device fabrication technology. This brings hope that very high efficiency silicon solar cells can be attained in the future when all the deleterious losses from extrinsic origin or crystal imperfections can be eliminated. A categorization of these recombination processes is given in the following table.

TABLE II
RECOMBINATION PROCESSES IN SOLAR CELLS

INTRINSIC MECHANISMS (Interband Transitions) *****	ENERGY EXCHANGE PARTNER (Energy Loss Mechanisms) *****
I.1 Thermal Recombination	Phonons (Lattice Vibration)
I.2 Radiative Recombination	Photons
I.3 Auger Recombination	Second Electron or Hole
EXTRINSIC MECHANISMS (Band-bound Transitions) *****	ENERGY EXCHANGE PARTNER (Energy Loss Mechanisms) *****
E.1 Thermal Recombination (SRH)	Phonons (Lattice Vibration)
E.2 Radiative Recombination	Photons
E.3 Auger Recombination	Second Electron or Hole

A main fundamental difference between the intrinsic and extrinsic recombination mechanisms is that the initial and final states of the electron or the hole are in different energy bands separated by a large energy gap in the intrinsic processes. The energy exchange or loss during one of the three intrinsic recombination processes is much larger than the largest phonon energy, about 60 meV for optical phonons in solids. Thus, except for the interband thermal recombination transition, I.1 listed in Table II, other methods must be employed to dissipate the recombination energy loss of an electron-hole pair. For example, in I.2, the radiative recombination process, the electron energy loss when dropped into a hole is carried away by a photon. In the interband Auger recombination transition, I.3, the energy loss is carried away by a second electron or second hole which is in the vicinity of the recombining electron-hole pair.

For the three extrinsic recombination mechanisms listed in Table II, the initial or final state of the recombining electron and hole is a localized or bound state located at a lattice imperfection, such as a chemical impurity or a physical defect (vacancy, divacancy, vacancy clusters and dangling bonds) or a complex involving many impurity atoms and vacancies. In contrast, the initial and final states of the electrons and holes in an intrinsic or interband recombination transition are the nonlocalized band states which extend over the entire crystal. The energy exchange in the extrinsic recombination transition covers a wide range from the small value of an acoustical phonon of a few meV to large values approaching that of the fundamental energy gap of an electron-volt or two.

Thus, the intrinsic mechanisms cannot be completely eliminated in solar cells although cell designs may be optimized to reduce the recombination rates via these intrinsic mechanisms which will be discussed in section 4. However, the extrinsic mechanisms can be reduced or even eliminated as the silicon device fabrication technology keeps advancing. It should be emphasized that the extremely low density requirement on the recombination center density over extremely large device or cell areas exceeds the capability of even the latest and most advanced silicon VLSI circuit fabrication technology.

Among the recombination processes listed in Table II, the intrinsic Auger and Radiative mechanisms pose the ultimate limit for greater than 20% AM1 cells which is elaborated in section 4. However, the extrinsic thermal recombination mechanism, the SRH or Shockley-Read-Hall process, accounts for the current technology limit. The recombination rate and loss of the SRH thermal recombination process is proportional to the density of the impurities and defects.

These imperfections can be unintentionally but readily introduced during the cell fabrication procedures and they may be present in the starting silicon crystal, being incorporated during crystal growth. Thus, this limiting factor of the current-best cells can be largely removed with anticipated advances in silicon integrated circuit fabrication technology.

3.2.2 RECOMBINATION SITES

These recombination processes can occur preferentially at certain regions or locations in a solar cell which suggests device design and technology innovations to reduce and eliminate them. A schematic illustration of the cross-sectional area of a p+/n/n+ solar cell is given in Fig.2. The cell can be described generally by a number of layers and interfaces where one or more of the recombination mechanisms may be important. The layers are: the quasi-neutral emitter, base and back-surface field layers; and the p/n junction space charge layer; and the interfaces: the oxide/silicon, metal/oxide and metal/silicon interfaces on the front and back surfaces illustrated in Fig.4(a).

Not all of the six recombination mechanisms are important in these layers. For example, in the highly-doped p+ emitter layer, only the interband Auger and the SRH recombination mechanisms may be important. The interband Auger mechanism can be important if the majority carrier density in the quasi-neutral emitter exceeds about 1×10^{17} hole/cm² or the emitter layer sheet resistance exceeds about 0.6 ohm/square [28] since the Auger recombination rate for the injected or photogenerated electrons in the p+ emitter layer is proportional to the square of the hole concentration.

For another example, the SRH mechanisms could also be important in the quasi-neutral p+ emitter if the density of the defect recombination centers in the emitter is greatly increased due to heavy doping of the p+ emitter by a

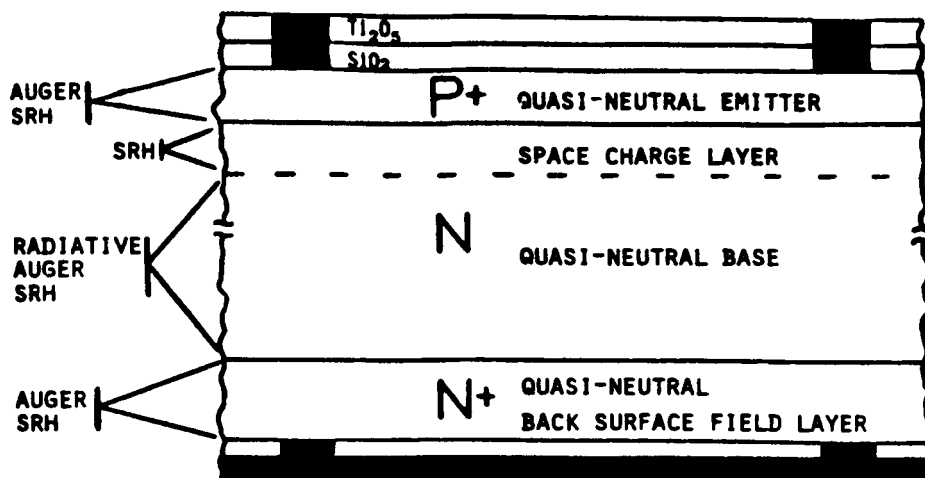


Fig.4(a) A cross-section view of solar cell showing the dominant recombination processes and locations. RADIATIVE and AUGER are the interband radiative and Auger recombination mechanisms. SRH is the Shockley-Read-Hall thermal recombination at defect and impurity recombination centers. Recombination occurs both in the bulk layers and at the interfaces between oxide, silicon and metal(dark).

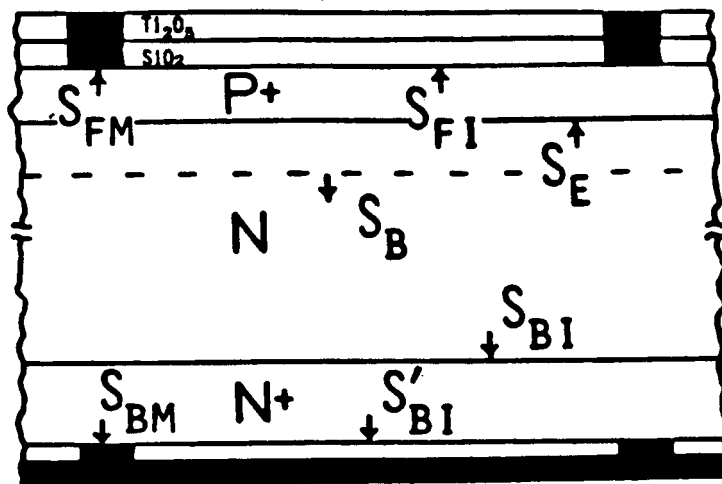


Fig.4(b) A cross-section view of solar cell showing the recombination velocity representation of the recombination rates. S_E , S_B and S_{BI} are the effective recombination velocities of volume recombination processes. S_{FI} , S'_{FM} , S'_{BI} and S'_{BM} are the real interface recombination velocities at the front oxide/silicon, front metal/silicon, back oxide/silicon and back metal/silicon interfaces.

high concentration of boron impurity. Heavy doping introduces localized band-tail states and broadens the boron impurity level into an impurity band, both of which give a narrowing of the energy gap. This energy gap narrowing will increase the minority carrier density appreciably by increasing the intrinsic carrier density, n_i . The higher minority carrier density would increase the dark current coefficient, J_1 , by the factor $\exp(\text{DEG}/kT)$ where DEG is the reduction of the energy gap which appears in n_i .

There has been no concrete evidence showing that the localized or band-bound Auger recombination process, E.3 in Table II, is important in the heavily doped emitter layer [29]. However, it is anticipated due to both the large majority carrier density and the high density of defects and dopant impurities.

In the quasi-neutral base layer, the interband or intrinsic radiative, the interband Auger, and the SRH localized recombination processes may all be important. In cells with less than 20%-AM1 efficiency, SRH losses at recombination centers will dominate while the interband radiative and Auger recombinations are not significant. When the extrinsic recombination losses, such as the SRH process in the quasi-neutral base and emitter layers and at the interfaces, are reduced or eliminated, the interband or intrinsic radiative and Auger recombination mechanisms become the limiting mechanisms. This is fully discussed in section 4 for very-high efficiency cells.

The analysis just made for the highly doped emitter layer can also be applied to the back-surface-field (BSF) layer. However, recombination in the BSF layer has much less influence on the cell performance than the emitter layer on the front surface since most of the electron-hole pairs are generated by light in the front surface region. The main requirement for the BSF is to

have a sufficiently low recombination rate and steep impurity gradient at the high-low junction so that most of the minority carriers are reflected back towards the front surface by the low/high junction interface. If the reflection is very efficient or 100%, then no photo-generated minority carriers can penetrate into the BSF layer to recombine with the majority carriers there. Then, the recombination loss in the BSF layer would have little influence on the dark recombination current J_1 .

Recombination of photogenerated minority carriers at the localized states in the interfacial layers on the front surface can significantly reduce and limit the efficiency by increasing the dark current J_1 . From analysis of the recently reported cells to be given in section 3.3 it is evident that some of these high-efficiency less-than-20% cells are somewhat limited by recombination losses at the front interfacial layers.

Recombination at exposed surfaces and interfaces can occur via the six mechanisms just described with the SRH recombination at interface and surface states being the most important and interband Auger mechanism very effective on highly-doped emitter surfaces. The recombination centers at the interfaces and surfaces are the dangling bond sites of silicon and oxygen arising from abrupt transition from a silicon lattice to an amorphous oxide or insulator structure. Extensive studies of these dangling bonds and their generation and annealing kinetics in the presence of hydrogen and high electric field as well as high densities of energetic electrons have been made and quantified [30,31]. The hydrogenation and dehydrogenation of these dangling bonds as well as the dopant acceptors (B, Al, Ga and In) [32-34] have been intensively investigated with extensive proof of the formation of the hydrogen bonds with the group-III acceptors [35].

In addition, the SRH mechanism is expected to be very effective at the contact-metal/silicon interface since this non-rectifying or ohmic Schottky barrier usually contains a high density of recombination centers. Latest clean oxidation technology has reduced the interface recombination losses at the oxide/silicon interface to a level which is unimportant in integrated circuit applications. However, the level may not be low enough for above 20% silicon solar cells. Recombination at the contact-metal/silicon interface mentioned above has also been a serious deterrent to high efficiency cells above 20%-AM1 efficiency. Even the recombination area of the low coverage contact fingers is small, the interfacial recombination rate at such a metal/silicon interface is so high that there could still be a significant net increase of the dark current, J_1 , from the recombination at this interface of the 'dark-diode' in the shades of the conductor fingers.

3.2.3 COMPARISON OF RECOMBINATION LOSSES BY EFFECTIVE RECOMBINATION VELOCITY

To estimate the recombination losses at the various bulk and interfacial layers just discussed, an effective interface or surface recombination velocity may be defined. This approach enables us to compare the contributions from the various regions and layers conveniently. The definition comes from the one-to-one relationship between the dark current, J_1 , and the interface or surface recombination velocity, S , at a true surface or interface. This is given by

$$I_1 = J_1 A = \sum_{m=1}^4 q S_m N_m A_m \quad (3.2.1)$$

where S_m is the effective surface or interface recombination velocity of minority carriers impinging onto the interface, N_m is the minority carrier density on its arrival side of the interface and A_m is the area of the surface or interface element. This is summed over all the surfaces, interfaces and arrival surface of the recombination volumes to give the total dark current, I_1 .

Fig.4(b) shows several effective and real interfacial recombination velocities in a solar cell. For example, SFI and SBI are the true recombination velocities at the front and back oxide/silicon interfaces. SFM and SMB are the true interface recombination velocities at the front and back metal-contact-to-silicon interfaces. However, SE, SB and SBI are the effective surface recombination velocities of the emitter, the base layer and the low/high n/n+ BSF junction layers.

One may readily obtain the following results by solving the minority carrier continuity and diffusion current equations, Eqs.(3.1.1) and (3.1.3) in the p-type region and Eqs.(3.1.2) and (3.1.4) in the n-type region, with the drift currents neglected.

$$J_1 = q \cdot n_E \cdot SE + q \cdot p_B \cdot NB \quad (3.2.2)$$

where

$$SB = (X_B/t_B) + SBI + SBA + SBO \quad (3.2.3)$$

$$SE = (X_E/t_E) + SFI + SEA + SEO \quad (3.2.4)$$

Here, X_B and X_E are the base and emitter layer thickness; t_B and t_E are the minority carrier lifetimes in the quasi-neutral base and emitter layers respectively. SBI and SFI are the effective and real recombination velocity at the back and front interfaces; SBA and SEA are the effective recombination velocities from volume interband Auger recombination in the quasi-neutral base and emitter layers respectively; and SBO and SEO are those from the volume interband radiative recombinations. These very simple expressions are applicable for base and emitter layers which are thin compared with the minority carrier diffusion lengths, a condition that holds well in high efficiency cell designs. The recombination velocities are given by

$$SBT = XB/tB \quad (\text{All Level SRH}) \quad (3.2.5)$$

$$SBA = C_L^a * XB * NB \quad (\text{Low Level Auger}) \quad (3.2.6)$$

$$SBA = C_H^a * XB * n_i^2 * \exp(qV/kT) \quad (\text{High Level Auger}) \quad (3.2.7)$$

$$SBO = C^o * XB * NB \quad (\text{All Level Radiative}) \quad (3.2.8)$$

for the base layer. A similar set holds also for the emitter layer.

Numerical values of the effective surface recombination velocities are computed for typical cells given in Table III for the simple SRH case from those cells given in Table I. In section 4, the Auger and radiative limits will be computed and discussed for the ultimate efficiency cells. It is evident from Table III that extremely low effective interface recombination velocities are required for cells with greater than 20%-AM1 efficiency. It is also evident that this value is strongly dependent on the majority carrier density at the interface or surface where the effective recombination velocity is computed. For example, for the 19.88% cell which is assumed to be limited mainly by base recombination, the effective base recombination velocity is 128 cm/s for a base doping of $1.0E16 \text{ cm}^{-3}$. Thus, emitter surface or interface recombination loss can be important only when the emitter interface recombination velocity is more than $12.8 * (NE/NB) = 1.28E+5 \text{ cm/s}$ if we assume that the emitter dopant density at the emitter surface is $1.0E+4$ times higher than the base doping. This value of emitter surface recombination velocity is so high that in practice emitter recombination cannot be too significant. However, in the calculation, Auger recombination and energy gap narrowing at the very highly doped emitter surface were not included. Energy gap narrowing alone can increase the minority carrier density at the surface by 10 or 100 times, reducing the emitter recombination velocity limit by the corresponding factors to $1.28E+4$ or $1.28E+3$, the latter would make the emitter interface recombination

loss significant. This is probably the case in some experimental cells whose efficiency decreased when the emitter surface oxide was removed since the bared emitter surface may have a very high surface recombination velocity, $1.E+6$ cm/s or higher on chemically etched surfaces.

3.2.4 EFFECTS OF OHMIC CONTACTS AND BACK-SURFACE FIELDS

Table III gives also an example which illustrates the importance of having a back-surface-field layer to reduce the effect of back surface recombination loss. This example arises from the question: can the back surface field layer be replaced by a thick base and the cell still have a very high efficiency? This is a practical question since the BSF layer requires extra cell fabrication steps at high temperatures which usually reduces the bulk lifetime in the quasi-neutral base. As a consequence, some of the best production cells to-date have AM1 efficiencies less than 17% due to the loss at the back contact from not having a highly effective BSF layer, whose designed theoretical efficiency exceeds 19%.

TABLE III
PERFORMANCE AND REQUIREMENT OF 20% SILICON BSF p+/n/n+ CELLS

•••Base Recombination Only•••

VOC mV	FF	EFF %	J_1 mA/cm ²	S_B cm/s	τ_B US	N_{TT} T1/cm ³
660	.8375	19.88	2.0E-13	128	39	1.7E12
680	.8410	20.56	9.4E-14	58	83	6.5E11
700	.8445	21.26	4.3E-14	27	186	3.6E11
720	.8460	21.90	2.0E-14	12	407	1.6E11
LIMITS		none	none	(a)	(b)	(c)

Legend: PIN=89mW/cm²; JL=32mA/cm²; 24.0C; (a) $S_E=0, P_E=10^{20}/10^{16}-1\Omega\text{-cm}$
 (a) S_B increases by 10X if N_B increases by 10X to 10^{17}cm^{-3} .
 (b) $S_{BI}=0; X_B=50\mu\text{m}$; (c) $c_p=1.5E-8\text{cm}^3/\text{s}; \tau_{Auger}=3.6\text{ms}$.

3.3 EVALUATION OF FOUR RECENT HIGH-EFFICIENCY CELLS

Silicon solar cells with efficiency approaching 20%-AM1 have been fabricated in the laboratory and 17%-AM1 in production [36]. Innovative cell designs have been developed to reduce interface and emitter recombination losses by Green [37] using a thin tunnel oxide layer between the contact metal fingers and the n-type emitter layer in a metal/insulator/n/p (M/I/N/P) cell structure to reach an efficiency greater than 19%. In this section, the experimental performance data of the best cells of four industrial laboratories are compared with that predicted by the ideal diode cell theory presented in subsections 3.1 and 3.2. From these comparisons, it appears that bulk recombination in the quasi-neutral base via the SRH mechanism through impurity and/or defect centers is the limiting loss on the three higher efficiency laboratory cells while the fourth cell design may be limited by recombination on the back surface. The experimental [36-40] and computed cell performance parameters are given in Table IV. One or more computed data are given to illustrate possible variation and uncertainty in the material (resistivity, mobility, lifetime, diffusion length) and geometry (length, width, junction depth) parameters among cells in a batch. The computed data is based on recombination at recombination centers in the base only but the effective recombination velocity are also given to gauge other possible mechanisms and locations of recombination.

The results of all four cells show that the experimental J_1 's can be almost completely accounted for by the computed J_1 using the measured base diffusion length or lifetime and resistivity data supplied by the authors. The predicted efficiency by the ideal diode cell theory, indicated by the Theory rows in Table IV, is smaller than the experiment in all four cells. The loss is

TABLE IV

PERFORMANCE OF FOUR HIGHEST EFFICIENCY SILICON SOLAR CELLS AND
COMPARISON WITH IDEAL DIODE CELL THEORY

SOURCE (type)author *****	RHO ohm-cm *****	THICK (μ m) *****	LB (μ m) *****	TAU (μ s) *****	J1 (A) *****	JSC (mA) *****	VOC (mV) *****	FF *****	EFF% AM1 *****	SB (cm/s) *****
(M/I/N/P)										
Ideal Theory	0.2		170		3.2E-13	36.0	660	0.840	20.0	850
Ideal Theory	0.2		170		6.6E-13	36.0	641	0.835	19.3	1750
Green Exp	0.2	280		20	3.2E-13	36.0	653	0.811	19.1	

(N+/P/P+)										
Ideal Theory	0.3			13	1.2E-12	36.2	627	0.834	18.9	1100
Spitzer Exp	0.3	380	150			36.2	622	0.801	18.0	
						35.9	627	0.800	18.1	

(N+/P/P+)										
Ideal Theory	4.0			23	2.0E-12	36.2	605	0.830	18.2	650
Rohatgi Exp	4.0	150	263		2.0E-12	36.2	605	0.786	17.2	
	0.2					36.0	627	0.800	18.1	

(N+/P)										
Ideal Theory	0.15				1.0E-12	36.0	628	0.834	18.9	2200
ASEC Exp	0.15					36.0	625	0.805	18.1	
	10.0					36.5	610	0.775	17.2	

Green: University of New South Wales, Australia.

Spitzer: Spire Corporation, Bedford, MA.

Rohatgi: Westinghouse R & D Center, Pittsburgh, PA.

ASEC: Applied Solar Energy Corporation, City of Industry, CA.

TABLE V

BASE DIFFUSION LENGTH AND BSF SURFACE RECOMBINATION VELOCITY DATA

SOURCE	TYPE	RHO ohm-cm	TBASE (um)	LB (um)	TAU (us)	SBI (cm/s)	JSC/AM1 (mA/cm ²)	VOC (mV)	EFF (%)
*****	*****	*****	*****	*****	*****	*****	*****	*****	*****
Neugroschel	N+/P/P+	10	227	450	(60)	105	-	-	-
Neugroschel	N+/P/P+	10	92	600	(103)	180	-	-	-
Neugroschel	N+/P/P+	1.5	220	600	(136)	380	38/AM0	617	-
Neugroschel	P+/N/N+	7.0	320	503	(200)	80	39/AM0	605	-
IdealTheory	P+/N/N+	0.6	50	320	39	(128)SB	36.0	660	20.0
Green	M/I/N/P	0.2	280	(170)	20	(850)SB	36.0	653	19.1
Spitzer	N+/P/P+	0.3	380	150	(13)	(1100)SB	36.2	622	18.0
Rohatgi	N+/P/P+	4.0	150	263	(23)	(652)SB	35.9	605	17.1
ASEC	N+/P	0.15				(2200)SB	34.8	620	17.1

Legend: Values in () are computed. All at AM1.5 except two AM0s and all 24C.

due to lower experimental fill factor, FF, than theory. This is likely to be due to series resistance not accounted for in the theory and it indicates that further design refinements of the metal contact grid lines may recover the remaining efficiency loss in the experimental cells.

The main conclusion from the comparison between the experimental data and ideal diode cell theory is that base recombination through defect and impurity recombination centers via the thermal or SRH mechanism is the limiting recombination loss mechanism in these four cells. Reduction of the series resistance will bring the fill factor and efficiency of the experimental cells up to the base-recombination limited values. Further improvement of the cell performance to efficiencies beyond the theoretical values given in Table IV, 18.2% to 20.0% at AM1, would require design improvement of the entire cell to reduce the base recombination losses further. Although the authors of these cells have reported efficiency reductions in test cells where the surface passivation oxide is removed, their highest-efficiency oxide-passivated cells probably had sufficiently low recombination losses in the emitter layer and at the oxide/emitter interface so that recombination losses in the base was the most probable remaining loss mechanism.

The contribution of the interface recombination at the back surface to the base recombination loss can be illustrated by the effective base recombination velocity, S_B , given in Table IV and a comparison of the experimental values. This comparison is given in Table V. Neugroschel's surface recombination data were obtained by a new method developed by him [41] which allowed a separation of the recombination loss in the quasi-neutral base from that at the back surface. He demonstrated this technique on many p/n junction solar cells.

Four of Neugroschel's surface recombination velocity measurements are listed in Table V. The base recombination was measured in terms of the base minority carrier diffusion length, L_B ; and the back surface recombination velocity, S_{BI} , in terms of the effective value at the low side of the low/high junction of the BSF layer. The effective total base recombination velocities, S_B shown in Fig.4(b) or Eq.(3.2.2), for the four high-efficiency cells given in Table IV are also tabulated in Table V for comparison with Neugroschel's data and with the ideal theory. Two points can be made. The effective total base recombination velocities of the four high-efficiency cells are significantly higher than the effective BSF layer recombination velocity measured by Neugroschel. This indicates that BSF recombination is not likely to be important in these four cells, although one would expect some contributions in the Green and ASEC cells which have no effective BSF layers. The second point to be made is that Neugroschel's data provide experimental confirmation that the effective BSF recombination velocity can be made quite low, as low as 80 cm/s. For this value of BSF recombination loss, an efficiency exceeding 20%-AM1 can be achieved.

IV. ANALYSES FOR ULTIMATE EFFICIENCY LIMIT

The ultimate performance is limited by the intrinsic recombination losses. Refined and stress-free clean fabrication technology can reduce and eliminate the recombination sites and hence the extrinsic recombination losses at these sites, but it cannot reduce the intrinsic losses. The fundamental intrinsic limits are due to the interband Radiative and Auger recombination mechanisms listed in Table I. The computed theoretical cell performances to illustrate the ultimate or fundamental limits are given in Table VI. They were obtained with certain assumptions as follows. All emitter recombination losses are assumed negligible. This is achievable by proper design of the emitter dopant concentration profile so that the total majority carrier density (carrier per area of the emitter layer) is less than about $1E14 \text{ cm}^{-2}$ [28,41] and there is an effective P+/P front surface field or high/low junction near the front surface of the emitter layer [42]. The assumption of negligible emitter recombination is not only a practical necessity to reach the ultimate efficiency but is also a valid assumption since for an ultimate cell, the base has to be thick to absorb most the light in order to give high photo- or short-circuit current. In addition, the base doping should be made high to reduce the minority carrier concentration in the base in order that thermal recombination rate of the minority carriers via the residual recombination centers in the base can be made negligible. These two conditions would increase the Auger and Radiative recombination in the base due to the thick base, while the former is further enhanced by the high base doping or high concentration of majority carriers in the base. SRH recombination loss decreases with increasing base doping while Auger recombination loss increases with increasing base doping, thus,

there is an optimum base doping for maximum efficiency. This optimum doping can be estimated from the dark current coefficient, J_1 , of the three mechanisms listed as follows:

Radiative Recombination (Interband)

$$J_1 = q \cdot C^o \cdot XB \cdot n_i^2$$

Auger Recombination (Interband)

$$J_{2/3} = q \cdot C^a \cdot XB \cdot n_i^3 \quad (\text{High Level})$$

$$J_1 = q \cdot C^a \cdot XB \cdot n_i^2 \cdot NB \quad (\text{Low Level})$$

Thermal Recombination (Bound-Band SRC)

$$J_1 = q \cdot \tau_B^{-1} \cdot XB \cdot n_i^2 / NB \quad (\text{Low Level})$$

$$J_2 = q \cdot \tau_B^{-1} \cdot XB \cdot n \quad (\text{High Level})$$

For the interband Auger recombination at high injection level, the diode law has a superlinear slope of 3/2 on a logI vs V plot. This superlinearity arises from the dependence of the interband Auger recombination rate on the product of the minority carrier density and the square of the majority carrier density, $C^p N^2 + C^n N^2 P$, since $N = P = n_i \exp(qV/2kT)$ when the base is at the high injection level condition.

Numerical calculations are made at 24C to illustrate the ultimate performance capability of silicon solar cells with an electrically active base layer thickness of $XB = 50$ microns. At 24C, $n_i = 1.0E10 \text{ cm}^{-3}$. The radiative recombination rate is taken to be $0.62E6$ for $C^o n_i^2$ while the interband Auger rates are: $C^n = 2.8E-31$ and $C^p = 0.99E-31 \text{ cm}^6/\text{s}$. To illustrate the condition at which the SRH recombination loss will begin to reduce the ultimate efficiency, a base lifetime of $100 \mu\text{s}$ and diffusivity of $20 \text{ cm}^2/\text{s}$ are assumed.

The results are tabulated in Table VI. This table also gives the performance of two ohmic-contact cells to illustrate the effect of surface and interface recombination on the ultimate efficiency.

Table VI shows that the ultimate efficiency is limited by both the Radiative and high level Auger recombination in the base. The maximum efficiency of this 50 um cell is about 25.4%-AM1. The high-injection level Auger recombination limited performance is reached if the majority carrier or doping impurity concentration in the 50-micron base is less than about $5E16 \text{ cm}^{-3}$ which gives a total majority carrier density of $2.4E14 \text{ cm}^{-2}$. Designing and operating the cell in the high-level Auger limited range by reducing the base doping may help in maintaining the high SRH recombination lifetime in the base which is necessary to achieve the high efficiency, but the sensitivity to surface recombination becomes more severe at this high injection levels, as indicated by the S_{EFF} data in Table VI and discussed later in this section.

Table VI also gives two cells which are limited by the SRH recombination processes in the base at both low and high injection levels. Two design ideas may be drawn. (1) High level injection should be avoided. This was arrived at previously by the observation that the high level recombination current law, $\exp(qV/2kT)$, gives a softer illuminated I-V curve and hence lower fill factor and efficiency. (2) Table VI also gives the condition at which SRC recombination loss will become important so as to significantly lower the ultimate efficiency. The example assumes a SRH recombination lifetime of 100 μs to give a 23%-AM1 efficiency. To reach 25%, the SRH base lifetime must be increased by 10 or to greater than about 1000 μs or 1 ms which is at the limit of the state-of-the art of current silicon VLSI technology.

Table VI also illustrates the importance of having a back surface field layer to reduce the effect of back surface recombination which is a must to reach the intrinsic or ultimate efficiency. We may again address the commonly asked question of whether the back-surface-field layer can be replaced by a

thick base in order to avoid the extra high temperature and lifetime reducing steps to fabricate the back-surface-field layer. This question may become more important in a ultimate limit cell design since recombination loss in such a cell comes from the minute intrinsic or interband Auger and Radiative recombination losses in the base. The expressions for the dark current, J1 and J2, without a BSF low/high junction and with an infinite back surface recombination velocity, are given by

$$\begin{aligned} \text{and } J1 &= q \cdot DB \cdot XB^{-1} \cdot (n_i^2 / NB) & SB=DB/XB & \text{(Low Level)} \\ J2 &= q \cdot DB \cdot XB^{-1} \cdot (n_i) & SB=DB/XB & \text{(High Level)} \end{aligned}$$

Suppose that we ask the question of what base thickness is required so that the of recombination loss from the infinite-recombination-velocity back surface is less than that from interband Auger recombination in the base. To answer this question quantitatively, we set the corresponding two J1's or recombination velocities equal. Consider the low level case, we have

$$XB \cdot C^a \cdot NB \cdot n_i^2 = DB \cdot n_i^2 / (NB \cdot XB)$$

or

$$NB \cdot XB = \text{SQRT}(DB/C^a) = \text{SQRT}(20/2.8E-31) = 1.0E+16 \text{ cm}^{-2}.$$

Thus, for a base doping of $NB=1.0E+17 \text{ cm}^{-3}$, have a base thickness of $XB=1000 \mu\text{m}$ or 1mm is required which not practical. This further demonstrates the importance of having an effective low/high junction or potential barrier near the back surface to shield the high-recombination rate back surface from the photo generated minority carriers.

In conclusion, the ultimate efficiency is reached when all the emitter recombination losses are eliminated and the extrinsic recombination via recombination centers in the quasi-neutral base on the back surface are

also eliminated. Then, the ultimate efficiency is limited by the interband Radiative and Auger recombination in the quasi-neutral base layer. It is desirable to maintain the low injection level condition in the base by high base doping but not to exceed the doping density at which Auger recombination in the base becomes comparable to the interband radiative recombination loss. Under this condition, the ultimate efficiency is about 25.4% in a cell whose active quasi-neutral base layer is 50-micron thick. The physical thickness of such a cell can be considerably larger in order to provide mechanical rigidity such as by ion implantation or epitaxial growth to achieve such a 50-micron thin active base layer. A thin active base is also advantageous for reducing recombination losses at the residual impurity and defect recombination centers in the base since their contributions to the dark current, J_1 , are minimized.

TABLE VI

ULTIMATE PERFORMANCE OF SILICON SOLAR CELLS
(Including the Effect of Surface Recombination)

SOURCE	J_1 (A)	J_{SC} (mA)	V_{OC} (mV)	FF	EFF (%)	m	J_1/q	S_{EFF} (cm/s)
Radiat. Recomb.	5.0×10^{-16}	36.0	817	0.8637	25.4	1	$C^O x_B n_i^2$	3.1
Auger H	3.0×10^{-22}	36.0	786	0.8968	25.4	2/3	$C^A x_B n_i^3$	0.33
Auger L	2.3×10^{-15}	36.0	776	0.8582	24.0	1	$C^A x_B n_i^2 N_B$	14
SRH L	8.0×10^{-15}	36.0	746	0.8540	23.0	1	$\tau_B^{-1} x_B n_i^2 N_B^{-1}$	50
Ohmic L	6.4×10^{-13}	36.0	634	0.8354	19.1	1	$D x_B^{-1} n_i^2 N_B^{-1}$	4000
SRH H	8.0×10^{-8}	36.0	666	0.7415	17.8	2	$\tau_B^{-1} x_B n_i$	50
Ohmic H	6.4×10^{-6}	36.0	442	0.6645	10.6	2	$D x_B^{-1} n_i$	4000

$T=24^\circ C$; $n_i=10^{10} \text{ cm}^{-3}$; Area= 1 cm^2 ; $x_B=50 \text{ } \mu\text{m}$; $N_B=10^{17} \text{ cm}^{-3}$; $D=20 \text{ cm}^2/\text{s}$;

$\tau_B=100 \text{ } \mu\text{s}$; $P_{IN}=100 \text{ mW(AM1.5)}$; L=Low Level; H=High Level;

$C^O n_i^2=0.62 \times 10^6$; $C_L^A=C^N=2.8 \times 10^{-31} \text{ cm}^6/\text{s}$; $C_H^A=C^N+C^P=3.8 \times 10^{-31} \text{ cm}^6/\text{s}$.

V. SUGGESTIONS FOR PRACTICAL SOLUTIONS

To achieve efficiency above 20%, all recombination losses must be reduced. The ideal diode cell calculation given in Table I indicated that the dark current coefficient, J_1 , must be less than 0.2 pA/cm^2 to reach 20% or higher AM1 efficiency. Base recombination loss must be reduced by the brute force approach of reducing the recombination center density. Some relaxation of this requirement could be made by using a thin active base with a highly effective low/high junction from the BSF layer. Such an approach of reducing base recombination has been demonstrated previously [16] with the additional use of an opposing drift field that retards the minority carrier diffusion towards the back surface. To further reduce the effect of back surface recombination, the back surface can be passivated by a thermal oxide since it is well known that the oxide/silicon interface has a very low recombination velocity if all the dangling silicon and oxygen bonds are removed either by slow annealing or by hydrogenation [30,31 and references therein]. The back contact will then have the metal stripe geometry similar to the front contact. Since the BSF layer can be made relatively thick, to be comparable to the minority carrier diffusion length in the BSF layer, metal stripes covering as much as 10% of the back surface could be sufficient to reduce the back surface and back contact recombination losses to a negligible level compared with other recombination losses. The low resistivity from larger metal conductor contact areas on the back surface of the silicon would insure low series resistance from this source. Thus, an optimum base design would be one with a relatively thin active base layer, about 50 to 100 microns, a very high base lifetime in the active layer, a built-in retarding field for the minority carriers in the base layer, an effective low/high junction at the back-boundary of the quasi-neutral base

layer, a not-too-highly doped BSF layer to reduce recombination loss in this layer and a relatively low recombination-velocity back silicon surface or interface such as that covered by a thermal oxide.

With these design considerations for the base, the remaining recombination loss would come from the emitter layer and emitter surface. Design considerations similar to those just discussed for the base and BSF layer can be used to design the emitter to reduce emitter recombination. However, the emitter is much thinner than the base and the emitter thickness is much less than the minority carrier diffusion length in the emitter in contrast to that in the base or the BSF layers. Thus, recombination losses at the interfaces on the front silicon surface will have a much larger effect on the dark current, J_1 , and on the efficiency than that at the back interfaces just discussed. Thus, highly effective oxide passivation of the silicon front surface over the emitter junction must be employed since a front high/low junction [42] to produce the retarding potential barrier against minority carriers is much more difficult to fabricate due to the thinness of the emitter layer. In addition, the recombination loss at the metal-conductor/emitter-silicon contact interface must be reduced since this dark contact diode could produce a very large dark current due to the very high recombination velocity at the metal/silicon interface, even when the front contact area of the fine grids may be only 1% of the total front surface area of a cell.

Green had approached this contact recombination loss problem by employing a thin tunneling oxide between the contact metal and the emitter silicon as indicated in Fig.4(b). However, uniform and thin tunneling oxides of less than 20 to 30 Å are difficult to grow reproducibly and its stability or reliability is expected to be rather poor, especially in view of the high-stress environment (high temperature and optical radiation) in which a solar cell must operate reliably over the lifetime of more than twenty years.

Another approach, proposed by this author at the 24-th PIM (Project Integration Meeting of JPL on October 2 and 3, 1984) [43], was to use a thin and doped poly-silicon barrier layer between the conductor metal and the heavily doped silicon surface of the emitter. Neugroschel [44] has measured the effective surface recombination velocity of the polySi/Si interface in very high speed VLSI bipolar silicon transistors with very shallow emitters. Table VII summarizes selected results. The solar cell performance data are computed assuming no base recombination loss and the unreal worse case which has the poly-silicon barrier over the entire front surface of the cell instead of just the contact areas. Even in this case, it is evident that the polysilicon barrier can significantly reduce the effective emitter/contact interface recombination velocity, to as low as 112 cm/s, giving a worse-case computed cell performance of 19.6%-AM1 efficiency. In reality, the front metal contact area is only about 1% of the cell area so that the effective recombination velocity would be reduced to 1.12 cm/s or J_1 reduced by 100X to $4.3E-15$ A/cm². This would give a VOC of 769mV, FF of 0.861 and an AM1.5 efficiency of 23.8%. This is still below the fundamental limit posed by the interband recombination in the base, giving further support on the importance of reducing all possible emitter recombination losses in order to attain the highest efficiencies.

In summary, one practical solution to achieve an AM1 or AM1.5 efficiency of greater than 20% is to employ a drift field in an efficient low/high junction BSF cell structure with relatively thin base such as 25 to 100 microns of epitaxial layer on a n+ substrate and with an oxide passivated emitter which has a polysilicon barrier between the contact metal and the emitter in the contact stripes. According to the available data on base lifetime and polyemitter contact recombination velocity, efficiency exceeding 20%-AM1 should be attainable.

TABLE VII

EFFECT OF A POLYSILICON BARRIER LAYER ON THE INTERFACE RECOMBINATION
VELOCITY OF A METAL-TO-HEAVILY DOPED SILICON EMITTER SURFACE

DEVICE NO.	BARRIER LAYERS	DOPING METHOD	HEAT TREATMENT	JPO (A/cm ²)	SFM (cm/s)	JSC (mA)	VOC (mV)	FF	EFF %
*****	*****	*****	*****	*****	*****	****	****	****	*****
-----NO BARRIER LAYER-----									
Metal	none		450C/20min	5. E-10	1.E6	36	468	0.795	13.4
-----SINGLE BARRIER LAYER-----									
1E	1500A	none	none	5.8E-10	1.E6	36	463		
1F	1500A	none	800C/64hr	5.5E-10	1.E6	36	465	0.794	13.3
1G	1500A	none	900C/5min	5.5E-10	1.E6	36	456		
1A	1500A	In-situ	none	9.2E-13	<240	36	630	0.835	18.9
1B	1500A	In-situ	800C/64hr	11.5E-13	<300	36	625		
1C	1500A	In-situ	900C/ 5min	8.5E-13	<221	36	632		
1D	1500A	In-situ	900C/15min	6.3E-13	<164	36	640	0.837	19.2
2BE	1500A	In-situ	1000C/15min	5.0E-13	<130	36	646		
-----DOUBLE BARRIER LAYERS-----									
1I	1500A 1000A	none In-situ	none	4.2E-10	1.E6	36	472	0.796	13.5
1J	Same as 1I	above	800C/64hr	4.3E-13	<112	36	650	0.838	19.6
1K	Same as 1I	above	900C/15min	4.2E-10	1.E6	36	472		
1L	Same as 1I	above	850C/64hr	4.6E-13	<122	36	648		
2BA	Same as 1I	above	750C/ 8hr	4.0E-10	1.E6	36	473		
-----THEORETICAL ESTIMATE-----									
Same as 1J with 1% front contact.				4.3E-15	<1.12	36	769	0.861	23.8

VI. SUMMARY AND CONCLUSION

In this paper we have presented an analysis to delineate the factors which may limit the current state-of-the-art crystalline silicon solar cells to less than 20% efficiency at AM1. We have also discussed the factors which may limit the ultimate efficiency and suggested practical designs which may break the 20% barrier. These factors are summarized in the following table, Table VIII.

To overcome the current 20% barrier, base recombination losses must be reduced in the reported cell designs. The highest-efficiency cell reported by Green [37] was not optimized to reduce base recombination. Further improvement of efficiency to more than 20% requires first an elimination of the large base recombination in the current cells by a novel graded-base back-surface-field thin base structure suggested by Sah and Lindholm [16] and then by a novel polysilicon barrier in the metal contact to emitter suggested also by Sah [43] and Lindholm. Estimated efficiency of such a structure could reach 23.8% (see Table VIII) which is near the intrinsic limit of 25% at AM1.

To reach the intrinsic or fundamental limit of 25.5% due to interband Auger and Radiative recombinations in the base, exceptionally clean and stress-free fabrication process technology must be developed and very long lifetime single-crystalline silicon (about one millisecond) must be used. The former is yet to reach the state-of-the-art stage and would require concentrated and further extensive development efforts, such efforts had been recognized first by the NAS-NRC Ad Hoc Panel on Solar Cell Efficiency in 1972 [7] and the Rappaport Workshop in 1973 [8].

TABLE VIII

SUMMARY OF EFFICIENCY LIMITING MECHANISMS

EFFICIENCY RANGE (%) *****	CURRENT STATUS *****	LIMITING MECHANISMS AND RECOMBINATION SITES *****	MAXIMUM DARK CURRENT J ₁ (A/cm ²) *****
25+	Must eliminate all emitter recomb. losses.	Interband Auger and radiative in base.	5.0E-16
20-24	Must reduce all base recomb. losses.	SRH at traps at the contact and oxide/silicon interface. Use polySi barrier for contacts.	2.0E-15 to 2.0E-13
18-20	Current best cells.	SRH at traps in the base layer.	2.0E-13 to 2.0E-12
<18	Current production.	SRH at traps in both the base and emitter.	>2.0E-12

VII. ACKNOWLEDGMENT

The author would like to thank Alan Yamakawa and Ralph Lutwack who started the author's profitable venture into crystalline silicon solar cell investigation on May 18, 1976, which has lasted for ten years through supports from the U. S. Department of Energy and the Jet Propulsion Laboratory. He is also indebted to Li-Jen Cheng, also of JPL, who succeeded Alan Yamakawa as the project manager for the thrust into the high efficiency crystalline silicon solar cell studies. The author is especially indebted to Mike Godlewski and Harry Brandhorst of NASA-Lewis, the former persuaded the author to take up a silicon solar cell research project on December 14, 1973. I wish also to thank Fred Lindholm who had accepted the NASA-Lewis grant at the University of Florida in 1974 when I could not due to lack of facility and prior commitments of graduate students, and who had been a source of continuous interaction during the last ten years.

VIII. REFERENCES

- [1] E. Becquerel, "Recollection on the electric effects produced under the influence of solar radiation," *Comptes Rendus*, 9, 561, Nov.4, 1839.
- [2] S. Bidwell, "Sensitiveness to light of selenium and sulphur cells," *The Chemical News & Journal of Industrial Science*, 52, 191, 1885.
- [3] D. M. Chapin, C. S. Fuller and G. L. Pearson, "A new silicon p-n junction photocell for converting solar radiation into electric power," *J. Appl. Phys.* 25, 676-677, May 1954. For a review, see also Paul Rappaport, "The photovoltaic effect and its utilization," *RCA Review*, 20, 373-397, September, 1959; and Martin Wolf, "Historical development of solar cells," *Proc. 25th Power Sources Symposium*, 120-124, May 23-25, 1972.
- [4] D. C. Reynolds and G. M. Leiss, "Light converted into electricity with Cadmium sulfide crystal," *Electrical Engineering*, 73(8), 734, August 1954; D. C. Reynolds, G. Leiss, L. L. Antes and R. E. Marburger, "Mechanism for photovoltaic and photoconductivity effects in activated CdS crystals," *Physical Review*, 96(2), 533, 15 October 1954. For a detailed review, see also Fred A. Shirland, "The history, design, fabrication and performance of CdS thin film solar cells," *Advanced Energy Conversion*, 6, 201-221, Oct.-Dec. 1966.
- [5] E. L. Ralph, "A plan to utilize solar energy as an electric power source," *Conference Record, 8-th IEEE Photovoltaic Specialist Conference*, 326-330, August 4-6, 1970.
- [6] C. G. Currin, K. S. Ling, E. L. Ralph, W. A. Smith and R. J. Stirn, "Feasibility of low cost silicon solar cells," *Conference Record, 9-th IEEE Photovoltaic Specialist Conference*, 363-369, May 2-4, 1972.
- [7] Report and Recommendations of the Ad Hoc Panel on Solar Cell Efficiency, from *SOLAR CELLS: Outlook for improved efficiency*, Chapter 1, p.3-22, (1972), Space Science Board, National Academy of Science, National Research Council, Washington, DC.
- [8] R. Rappaport, "Single-crystal silicon," *Proc. Workshop on Photovoltaic Conversion of Solar Energy for Terrestrial Applications*, Vol. 1, 9-16, October 23-25, 1973.
- [9] Charles, E. Backus, editor, *SOLAR CELLS*, IEEE Press, New York, 1976.
- [10] C. Tang Sah, "High efficiency crystalline silicon solar cells," *Second Technical Report*, JPL Publication DOE/JPL-956289-84/1, December 1984.
- [11] C. T. Sah, "Study of the effects of impurities on the properties of silicon materials and performance of silicon solar cell," April 1978, *Technical Report No. DOE/JPL-954685-78/1*, Jet Propulsion Laboratory.
- [12] *ibid.* March 1979. *Technical Report No. DOE/JPL-954685-79/1*.

- [13] ibd. February 1980. Technical Report No. DOE/JPL-954685-80/1.
- [14] ibd. March 1981. Technical Report No. DOE/JPL-954685-81/1.
- [15] ibd. October 1981. Technical Report No. DOE/JPL-954685-81/2.
- [16] C. T. Sah, "Study of relationships of material properties and high efficiency solar cell performance on material composition," First Technical Report, July, 1983, DOE/JPL-956289-83/1, Jet Propulsion Laboratory; see also C. T. Sah and F. A. Lindholm, "Performance improvements from penetrating back-surface field in a very high efficiency terrestrial thin-film crystalline silicon solar cell," J.Appl.Phys.v55(4),1174-1182, 15 February 1984.
- [17] C. T. Sah, P.C.H.Chan, C.K.Wang, R.L.Sah, K.A.Yamakawa and R.Lutwack, "Effect of zinc impurity on silicon solar cell efficiency," IEEE Trans. on Electron Devices, vED-28(3), pp.305-315, March 1981.
- [18] C. T. Sah, K.A.Yamakawa and R.Lutwack, "Reduction of solar cell efficiency by edge defects across the back-surface-field junction: - a developed perimeter model," Solid-State Electronics, v25(9),851-858,September 1982.
- [19] C. T. Sah, K.A.Yamakawa and R.Lutwack, "Reduction of solar cell efficiency by bulk defects across the back-surface-field junction," J.Appl.Phys. v53, (4), pp.3278-3290, April 1982.
- [20] C. T. Sah, K.A.Yamakawa and R.Lutwack, "Effect of thickness on silicon solar cell efficiency," IEEE Trans.Electron Device, vED-29(5), 903-908, May 1982.
- [21] C. T. Sah, "Thickness dependences of solar cell performance," Solid-State Electronics, v25(9), pp.960-962, September 1982.
- [22] C. T. Sah, "Equivalent circuit models in semiconductor transport for thermal, optical Auger-impact and tunneling recombination-generation-trapping processes," phys.stat.sol.(a),v7,pp.541-559, 16 october 1971.
- [23] Hermann Maes and C. T. Sah, "Application of the equivalent circuit model for semiconductors to the study of Au-doped silicon p-n junctions under forward biase," IEEE Trans. vED-23 (10), 1131-1143, 01 October 1976.
- [24] Philip C. H. Chan and C. T. Sah, "Exact equivalent circuit model for steady-state characterization of semiconductor devices with multiple-energy-level recombination centers," IEEE Trans. Electron Devices, vED-26 (6), 937-941, June 1979; "Experimental and theoretical studies of I-V characteristics of zinc-doped silicon p-n junctions using the exact DC circuit model," ibd. 937-941; "Computer-aided study of steady-state carrier lifetimes under arbitrary injection conditions," Solid-State Electronics, v22, 921-926, 1979.

- [25] M. B. Prince, "Silicon solar energy converters," J. Applied Physics, v26(5), 534-540, May 1955.
- [26] C. T. Sah, "Effects of surface recombination and channel on p-n junction and transistor characteristics," IRE Trans. Electron Devices, vED-9(1), 94-108, January 1962.
- [27] C. T. Sah, "Prospects of amorphous silicon solar cells," JPL Publication JPL/DOE-660411-78/01, 87pp. 31 July 1978.
- [28] C. Tang Sah, "Barriers to achieving high efficiency," Proceeding of the 23rd Project Integration Meeting held on March 14-15, 1984, PROGRESS REPORT 23, Jet Propulsion Laboratory, pp.123-130, JPL Publication 84-47.
- [29] P. T. Landsberg, private communication.
- [30] C. T. Sah, J.Y.C.Sun and J.J.T.Tzou, "Study of atomic models of three donor-like traps on oxidized silicon with aluminum gate from their processing dependences," J.Appl.Phys. v54(10), 5684-5879, October 1983.
- [31] C. T. Sah, J.Y.C.Sun and J.J.T.Tzou, "Study of atomic models of three donor-like defects in silicon metal-oxide-semiconductor structures from their gate material and process dependencies," J.App.Phys. v55(6), 1525-1545, 1 March 1984.
- [32] C. T. Sah, J.Y.C.Sun and J.J.T.Tzou, "Generation-annealing kinetics and atomic models of a compensating donor in the surface space charge layer of oxidized silicon," J.Appl.Phys. v54(2), 944-956, February 1983.
- [33] C. T. Sah, J.Y.C.Sun and J.J.T.Tzou, "Deactivation of the boron acceptor in silicon by hydrogen," Appl.Phys.Lett. v43(2), 204-206, July 15, 1983.
- [34] C. T. Sah, J.Y.C.Sun, J.J.T.Tzou and S.C.S.Pan, "Deactivation of group-III acceptors in silicon during keV electron irradiation," Appl.Phys.Lett. v43(10), pp.962-964, 15 November 1983.
- [35] C. T. Sah, S.C.S.Pan and C.H.C.Hsu, "Hydrogenation and annealing kinetics of group-III acceptors in oxidized silicon," J. Appl. Phys. 57(12), 5148-5161, 15 June 1985.
- [36] J. B. Milstein and C.R. Osterwald, "High efficiency solar cell program: some recent results," 23rd Projection Integration Meeting, March 14-15, 1984; Jet Propulsion Laboratory Publication 84-47, pp.151-157. J. B. Milstein, "Rapid advances reported in silicon solar cell efficiency," IN REVIEW (A SERI Research Update), VolVI(3), p.5, March 1984. Solar Energy Research Institute, Golden, CO.
- [37] Martin A. Green, A.W.Blakers, J.Shi, E.M.Keller, and S.R.Wenhan, "High-efficiency silicon solar cells," IEEE Trans. vED-31(5), 679-683, May 1984.

- [38] Mark B. Spitzer, S.P.Tobin, C.J.Keavney, "High-efficiency ion-implanted silicon solar cells," IEEE Trans. vED-31(5), 546-550, May 1984.
- [39] Ajeet Rohatgi and P. Rai-Choudhury, "Design, fabrication and analysis of 17-18 percent efficient surface-passivated silicon solar cells," IEEE Trans. vED-31(5), 596-601, May 1984; Ajeet Rohatgi, "Process and design considerations for high-efficiency solar cells," Proceedings of the Flat-Plate Solar Array Project Research Forum on High-Efficiency Crystalline Silicon Solar Cells, 429-446, JPL Publication DOE/JPL-1012-103, May 15, 1985.
- [40] Applied Solar Energy Corporation solar cells reported by Milstein in reference 36 and by Rohatgi in reference 39.
- [41] C. Tang Sah, "Recombination phenomena in high efficiency silicon solar cells," Proceedings of the Flat-Plate Solar Array Project Research Forum on High-Efficiency Crystalline Silicon Solar Cells, July 9-11, 1984, pp.37-52, DOE/JPL-1012-103, JPL Publication 85-38, 15 May 1985, Jet Propulsion Laboratory, Pasadena, CA
- [42] C. T. Sah, F. A. Lindholm and J. G. Fossum, "A high-low junction emitter structure for improving silicon solar cell efficiency," IEEE Trans. on Electron Devices, vED-25(1), 66-67, January 1978.
- [43] C. Tang Sah, "Important loss mechanisms in high efficiency solar cells," Proceeding of the 24th Project Integration Meeting, held on October 2-3, 1984, PROGRESS REPORT 24, pp.347-352, DOE/JPL-1012-104, JPL Publication 85-27, Jet Propulsion Laboratory, Pasadena, CA.
- [44] Arnost Neugroschel, presented by C. T. Sah at the 24th Project Integration Meeting of the Jet Propulsion Laboratory, October 2-3, 1984, Progress Report 24, pp.283-294, DOE/JPL-1012-104, JPL Publication 85-27.
- [45] A. Neugroschel, M. Arienzo, Y. Komem and R.D. Issac, "Experimental study of the minority-carrier transport at the polysilicon-monosilicon interface," IEEE Trans. Electron Devices, ED-32(4), 807-816, April 1985.